Expansion breccias in Lower Cretaceous Apennine pelagic limestones: II. Geochemical constraints on their origin

Belza, Joke; Alvarez, Walter; Tavarnelli, Enrico; Vanhaecke, Frank; Baele, Jean-Marc; Claeys, Philippe

Published in:
250 Million Years of Earth History in Central Italy: Celebrating 25 Years of the Geological Observatory of Coldigioco

DOI:
10.1130/2019.2542(13)

Publication date:
2019

Document Version:
Accepted author manuscript

$^{87}Sr/^{86}Sr$ RECORD FROM THE LOWER CRETACEOUS PELAGIC MAIOLICA LIMESTONE (CENTRAL APENNINES, ITALY) AND ITS OFFSET FROM THE GLOBAL SEAWATER REFERENCE CURVE

J. Belza[1*], W. Alvarez[2], F. Vanhaecke[1], P. Claeys[3]

[1]Department of Chemistry, Atomic and Mass Spectrometry (A&MS) research unit, Ghent University, Campus Sterre, Krijgslaan 281 – S12, 9000 Ghent, Belgium,

[2]Dept. Earth and Planetary Science, University of California Berkeley, CA 94720-4767 USA, and Geological Observatory of Coldigioco, Contrada Coldigioco, 62020 Frontale di Apiro, Italy,

[3]Dept. Analytical Environmental and Geo-Chemistry (AMGC), Vrije Universiteit Brussel, Pleinlaan 2 1050 Brussels, Belgium

Corresponding author: jbelza@vub.ac.be

ABSTRACT

This study provides a composite record of $^{87}Sr/^{86}Sr$, $\delta^{18}O$ and $\delta^{13}C$ for three sections in the Tethyan Lower Cretaceous Maiolica formation, a pelagic limestone from the Umbria-Marche Apennines of Italy, carefully tied to a magnetostratigraphically and biostratigraphically calibrated timescale. Although the $^{87}Sr/^{86}Sr$ record accurately follows the trend of the globalmarine $^{87}Sr/^{86}Sr$ reference curve , individual Sr isotope ratio values are relatively high for their inferred stratigraphic position, with all $^{87}Sr/^{86}Sr$ ratiosyielding a fairly uniform +0.00007

to +0.0001 discrepancy. This offset likely results from incorporation of excess ^{87}Sr through isotopic re-equilibration with interstitial pore waters during progressive lithification of the calcareous ooze. Although the process occurs principally through dissolution-reprecipitation, buffering the contemporaneous seawater Sr isotopic signature, diffusive communication with the overlying water column and porous sediments will compete with the dissolution-precipitation process, homogenizing pore fluid concentrations and isotope ratios throughout the sediment column. Because the secular trend in $^{87}Sr/^{86}Sr$ throughout the Maiolica timeframe is one of constant increase before rebounding to lower $^{87}Sr/^{86}Sr$ ratios in the Barremian, the ratios of the Maiolica carbonates are systematically displaced from that of the seawater in which it was deposited towards more radiogenic (higher $^{87}Sr/^{86}Sr$) values. In addition, the carbon and oxygen isotope record of the Maiolica allows identification of the Mid-Valanginian Weissert event, characterized by a positive excursion in the $\delta^{13}C$ and the $\delta^{18}O$ record. Furthermore, the Weissert event correlates with a positive spike (+0.0001) in $^{87}Sr/^{86}Sr$, Both the Sr and O isotopic peak signal pre-date the maximum peak in the $\delta^{13}C$ excursion. This is likely a diagenetic artefact and may support the hypothesis of diffusive communication during lithification of the calcareous ooze.

1. INTRODUCTION

1.1 The Umbria-Marche sequence

The stratigraphic sequence of the Umbria-Marche Apennines in central Italy offers a world-class archive of information about Earth history from the Pliensbachian, in the early Jurassic, to the Miocene in the Neogene (Cresta et al., 1989; Montanari and Koeberl, 2000; Alvarez, this volume). This is due to the pelagic character of these limestones, marls, and cherts, which were deposited on the thinned, subsided Italian continental crust at moderate oceanic depth, just above or just below the calcite compensation depth. Because of these conditions, the Umbria-Marche sequence lacks terrigeneous inputs until the Oligocene, is free of wave erosion, and was rarely affected by current scour. Equivalent pelagic oozes have been cored by scientific drilling ships at many sites throughout the world ocean, where they have the advantage of not having been compacted, uplifted, or placed in contact with non-marine pore waters. In compensation, the Umbria-Marche carbonate rocks are extensively exposed across whole mountain sides in a region of broad anticlinal folds covering about 5,000 km^2, so that lateral relationships can be studied and two-dimensional sampling can be carried out, neither of which is possible with deep-sea cores. Because pelagic carbonate rocks have usually either stayed at depth below the sea or been strongly deformed during tectonism and uplift, the Umbria-Marche Apennines are ideal for the study of pelagic carbonates in outcrop.

The great majority of stratigraphic research in the Umbria-Marche Apennines has focused on the ca. 600 m thick Scaglia formations — the Scaglia bianca, rossa, variegata, and cinerea — beginning with white pelagic limestone in the Cenomanian, then pink pelagic limestone from the Turonian to the Eocene, and transitioning to a grey pelagic marl in the Oligocene. The

Scaglia has been of great stratigraphic use because of the abundance of recognizable lithologic contacts and marker beds and of planktic foraminifera, and has led to advances in magnetic polarity stratigraphy, radioisotopic dating of intercalated volcanic ash beds, isotopic stratigraphy, event stratigraphy, including recognition of the Cretaceous-Palaeogene boundary impact event, and cyclostratigraphy (Coccioni and Montanari, this volume).

Turning to the Lower Cretaceous, less attention has been paid to the Aptian-Albian Fucoid marls (Grippo et al., 2004). The Tithonian-to-Albian Maiolica limestone (Sprovieri et al., 2006) has been particularly intractable, because of the 1) 400 m thickness of uniform lithology of white limestone with beds and nodules of black chert, 2) the presence of only a single recognizable marker bed, and 3) the absence of the planktic foraminifera, which had not yet evolved. Although the Maiolica yields good palaeomagnetic directions, magnetic-polarity stratigraphy has been difficult to apply to the Maiolica because the M-sequence reversals, covering almost all of the Maiolica, contain many short polarity zones with no distinctive long zones, making it hard to correlate a particular set of polarity zones in the Maiolica to the M-sequence reversals (Lowrie et al., 1980).

The overall architecture of the Maiolica shows a division into basinal sequences, typically ~400 m thick, and thinner sequences, ~100 m thick, on the tops and margins of fault-block seamounts (Alvarez, 1989). The seamount sequences are incomplete because of stratigraphic hiatuses, and in compensation, the basinal sequences commonly contain frequent levels of slumps. In the present paper we report on the study of one seamount and two basinal sequences.

The present study began with an attempt to use $^{87}Sr/^{86}Sr$ ratios as a correlation tool for the Maiolica. Specifically it aimed at providing a detailed stratigraphic framework to investigate

near-vertical walls of shattered breccia in the Maiolica formation, for which a hydraulic fracturing mechanism seems likely. In two companion papers (Alvarez et al., this volume; Belza et al., this volume), we detail the structural observations and geochemistry of these breccia walls, which are exposed along the anticlines of the Umbria-Marche Apennines thrust-and-fold belt. The breccias are mostly confined to the Maiolica formation, and are characterized by bodies of shattered pelagic limestone. Our goal was to determine, using $^{87}Sr/^{86}Sr$ ratios, whether the Maiolica breccia fragments have moved up or down, and how far, relative to the stratigraphic level where they now reside. The standard global marine $^{87}Sr/^{86}Sr$ reference curve (McArthur et al., 2012, Fig. 7.2) shows a monotonic rise from ~0.70715 to ~0.70750 in the first 80% of the Maiolica, followed by a decrease to ~0.70740 at the top of the formation. The long monotonic increase gave reason for hope that the strontium isotope ratio values in breccia fragments could identify their original stratigraphic position.

First, however, it would be necessary to test whether the Maiolica accurately records the global strontium-isotope reference curve for the Lower Cretaceous. The present study was undertaken to do this testing, and it unexpectedly showed that the $^{87}Sr/^{86}Sr$ values in the Maiolica, although they show the same pattern of a long rise followed by a shorter fall, are systematically offset by about +0.0001 relative to the global curve. Thus, our attempt to study the origin of the Maiolica breccias has been diverted into an attempt to understand the offset in the Maiolica strontium isotope ratio curve.

Our attempt to tie the $^{87}Sr/^{86}Sr$ record to the global Sr seawater reference curve was only possible because of the unique stratigraphic control of the sections studied: the pelagic limestones in the Umbria-Marche Apennines have been extremely well dated because of 1) the presence of microfossils and nanofossils 2) magnetic minerals recording the geomagnetic

polarity3) and the presence of levels of distal volcanic ejecta that can be dated radiometrically, which made it possible to tie all three major geological dating methods in one sedimentary succession (Alvarez, 2009). As such the stratigraphic positions of our samples were accurately determined by tying them to the magnetic polarity stratigraphy (Channel et al., 1995; Lowrie and Alvarez, 1984) and biostratigraphy (Cecca et al., 1994, Fig. 2, column 22; Faraoni et al., 1997 Coccioni et al., 1998). This was accomplished by identifying the old paleomagnetic drill holes in the succession and using the core orientations provided James E. Channel (personal communication).

1.2 Chemostratigraphy

Changes in ocean chemistry are controlled by fluctuating global weathering rates, by changes in volcanic and hydrothermal activity and by sedimentological and tectonic processes (Weissert et al., 2008). The variation in the past composition of seawater over geological time is recorded in the $\delta^{13}C$, $\delta^{18}O$, $^{87}Sr/^{86}Sr$ ratios of marine carbonates, and serves as a reliable stratigraphic tool for global correlation. In addition, the Sr, O and C isotopic signatures are useful in constraining post-depositional diagenetic events, an important factor that may obscure the targeted stratigraphic resolution. This is especially relevant for the oxygen isotopic system, as the $\delta^{18}O$ of the carbonate depositing from the fluid is temperature-dependant.

1.2.1 Carbon Isotope Ratio Stratigraphy

Because the $\delta^{13}C$ of carbonate is relatively insensitive to changes in temperature, the $\delta^{13}C$ isotopic signature of inorganically and biologically precipitated carbonate will reflect the (fractionated) $\delta^{13}C$ of dissolved inorganic carbon (DIC) of seawater at the point of calcification and can be used to trace changes in ocean circulation and palaeoproductivity (Zeebe and Wolf-

Gladrow, 2001; Edgar et al., 2013). The $\delta^{13}C$ value of whole-ocean DIC has not been constant over geologic time. Variations in $\delta^{13}C$ in the DIC in the oceans over time reflect redistribution of carbon among the Earth's surface carbon reservoirs such as the atmosphere, oceans, biosphere and lithosphere (Sundquist and Visser, 2003). This includes factors driven by changes in atmospheric CO_2 or DIC levels in the ocean, such as changes in bioproductivity and organic carbon burial.

1.2.2 Oxygen Isotope Ratio Stratigraphy

Oxygen isotope ratios in marine carbonate vary as a function of both the temperature and the $\delta^{18}O$ composition of the parent seawater (; Shackleton, 1967). The strongly temperature-dependent calcite-water oxygen isotope fractionation has been well-established by numerous empirical, experimental and theoretical studies. Increasing temperatures shift $\delta^{18}O$ values in marine calcite to more negative values. Combined with palaeontological information, $\delta^{18}O$ values serve as a reliable proxy for changes in palaeo-ocean temperatures, salinity, and global ice volumes (Shackleton, 1967; Veizer et al., 1986; Rohling and Bigg, 1998; Veizer et al., 1999; Edgar et al., 2013). As ocean temperatures vary with depth and latitude, oxygen isotope records will depend on palaeogeography and depth habitat of the calcifying microorganisms (Grossman, 2012).

Because the oxygen and carbon isotope signals in this study were measured on bulk carbonates, they might be sensitive to changes in the community of carbonate producers and diagenesis. This will be highlighted in the Discussion section.

1.2.3 Strontium Isotope Ratio Stratigraphy

The $^{87}Sr/^{86}Sr$ value of seawater has been recognized to be a diagnostic tool for stratigraphic correlations, reconstruction of global tectonics, palaeo-climatic perturbations, and

understanding of diagenetic processes (Burke et al., 1982; Veizer, 1989; McArthur et al., 2001; McArthur et al., 2012). The principle of strontium isotope ratio stratigraphy relies on the fact that the Sr isotopic composition of the oceans has varied throughout geological time, due to variation of two main sources contributing Sr to the oceans: (1) hydrothermal exchange of seawater with volcanic rocks on the ocean floor (Frijia and Parente, 2008), and (2) diagenesis and continental weathering of old marine limestones and weathering of old granitic rocks delivering strontium to the oceans by river influx (Faure and Powell, 1972)

Because the residence time of Sr in the oceans (10^6 years) is much longer than the time it takes currents to mix the oceans (10^3 years), oceans are thoroughly mixed on time scales that are short relative to the rates of gain and loss of strontium. As a result, the isotopic composition of strontium is considered to be constant throughout the global ocean at any one time (Veizer 1989; Palmer and Edmond, 1989). Because Sr^{2+} substitutes for Ca^{2+} during precipitation of marine carbonates and sulphates with minor isotope fractionation, the $^{87}Sr/^{86}Sr$ ratio of marine carbonates will reflect the isotopic ratio of the contemporary seawater during precipitation (Faure and Powell, 1972,.). Based on this assumption, Howarth and McArthur (1997) and McArthur et al. (2001) have compiled $^{87}Sr/^{86}Sr$ data and fitted to them a nonparametric LOWESS statistical regression function (Locally, Weighted Scatterplot Smoother), resulting in a global strontium seawater reference curve (McArthur et al., 2012).

With carbon isotope ratio data providing information on the evolution and perturbation of the global carbon cycle, and $\delta^{18}O$ isotope data, combined with palaeontological information, potentially serving as a palaeotemperature proxy (Weissert and Erba, 2004), the combination with strontium isotopic data provides a powerful chemostratigraphic tool to constrain the link between (continental) weathering, volcanism, tectonics and palaeoclimatic perturbations, and

document the temporal response of different isotopic systems on the Tethys carbonate sedimentation to the environmental perturbations.

1.3 Sections sampled

Most of the detailed sampling of Umbria-Marche pelagic limestone formations over the years has been done along roads because of the long, continuous sections, the fresh outcrops, and the exposure of easily erodible marl and shale layers (Lowrie et al., 1980; Alvarez et al.; 1977, Lowrie and Alvarez, 1977; Cecca, 1994; Cecca, 1995; Alvarez, 2009; Coccioni and Montanari, 2018) There are many such road-cut sections of the Scaglia, notably the Bottaccione and Contessa sections at Gubbio (several papers in this volume). The Maiolica offers fewer such usable sections; we have studied three of those available. The Monte Acuto (MMA) and Frontale (FRO) sections expose parts of the thick, basinal facies Maiolica, while the Presale (PRE) section exposes the thin, seamount facies. Sample localities are shown in Fig. 1.

1.3.1 Monte Acuto section (MMA)

The Monte Acuto section (MMA in this paper), located along the road from Chiaserna up to the pass between Monte Acuto and Monte Catria, exposes the lower 240 m of the Maiolica, with the upper part covered (Fig. 2). The complete stratigraphic record of the section extends from the middle Berriasian to the upper Hauterivian. Three thin black shale layers occur interbedded within the limestone beds (Sprovieri et al., 2006). The Maiolica sequence at the Monte Acuto section is cut by calcite-filled veins.

This excellent section represents the thick, basinal Maiolica, and it has been important for previous stratigraphic research on the Maiolica. The magnetic polarity stratigraphy together

with ammonite and nannofossil biostratigraphy were studied by Channell et al. (1995), the rare ammonites by Cecca (1995) and Faraoni et al. (1997), and the cyclostratigraphy by Sprovieri et al. (2006).

In October 2012, we collected 24 samples, from MMA-1 (at the lowest road elevation, but highest in the stratigraphy, at 43°27'49.80"N, 12°40'16.17"E), to MMA-24 (at the highest road elevation, but lowest in the stratigraphy, at 43°27'50.52"N, 12°40'44.70"E; coordinates from Google Earth, not from GPS). Our sample sites are marked with small numbers in green paint. The positions of our samples MMA-1 to MMA-10 have been tied to the magnetic polarity stratigraphy of Channell et al. (1995) and thus dated, based on identifying the palaeomagnetic drill holes, using the core orientations supplied by James E. Channell (personal communication, 2013). Stratigraphically, below MMA-10 there is a 20-30-m-wide covered interval which marks the bottom of the palaeomagnetic section of Channell et al. (1995).

In subsequent work by Faraoni et al. (1997) and Sprovieri et al. (2006), a prominent chert marker bed was recognized on both sides of the covered interval and painted blue, making it possible to continue the section downward below the base of the palaeomagnetic section, and this lower part of the section was tied to the global biostratigraphy using very rare ammonites Faraoni et al. (1997). Our samples MMA-11 to MMA-24 were taken in this lower part of the section, and were dated using the biostratigraphy of Faraoni et al. (1997).

1.3.2 Frontale section

A second section was sampled on the road from Frontale to Pian dell'Elmo. This basinal Maiolica was well exposed when the road cuts were fresh and was used for a palaeomagnetic stratigraphy study by Lowrie and Alvarez (1984). Sometime in the 30 years since that study,

the road cuts were covered by heavy screening. During the screening work, many core holes were cut away, and subsequently many others were covered by debris trapped behind the screen. However, we were able to identify enough of the remaining cores holes by their orientations (data from William Lowrie, personal communication, 2013) to re-measure the original section, confirming the location of two faults noted by Lowrie and Alvarez (1984). The meter levels of the recovered section have now been marked with green paint on the outcrop behind the screen, and on the metal guardrail on the opposite side of the road.

We took 23 samples for isotopic analysis, numbered with their meter levels, from FRO-470 (at the highest road elevation, but lowest in the stratigraphy, at 43° 20.949'N, 13° 5.055'E), to FRO-597 (at the lowest road elevation, but highest in the stratigraphy, at 43° 20.885'N, 13° 5.348'E; coordinates from Google Earth, not from GPS). Because of the presence of two prominent faults in the section (Lowrie, 1984— the "Big Fault" and the "Culvert Fault," the latter with its lowest exposure at a road culvert — not all of the samples were useful for the present stratigraphic study. The useful samples are FRO-470 through FRO-561, located in the long, unfaulted lower part of the section, which is dated by the magnetic polarity zones of Lowrie and Alvarez (1984), and FRO-565, 566, and 568, located in the block between the two faults, datable because it contains the upper Hauterivian Faraoni level (Cecca et al., 1994, Fig. 2, column 22; Coccioni et al., 1998).

1.3.3 Presale section

Since neither the Monte Acuto nor the Frontale section extends to the top of the Maiolica, we also sampled the Presale section, which seems to have been studied previously only by Lowrie and Alvarez (1984). This section is exposed along a trail 3.15 km southeast of the bridge at the main road junction in Piobbico. We were able to relocate several of the original painted

numbers corresponding to every 5 m in the 1984 magnetic stratigraphy section, although these green numbers are very faded and hard to see. Also recognizable are some of the supplementary green-painted meter marks (a line and 1, 2, 3, or 4 dots, corresponding to that many meters above a painted number).

We collected 10 samples, from the stratigraphically lowest, PRE-1 (43° 34.159'N, 12° 32.295'E, 170 m in the 1984 section), to PRE-10 (43° 34.195'N, 12° 32.346'E, 260 m in the 1984 section; coordinates from Google Earth, not from GPS). These samples are well dated because they are tied to the polarity stratigraphy of Lowrie and Alvarez (1984). It should be noted that the Presale Maiolica section is only about 100 m thick, which is typical of the thin Maiolica on the Jurassic fault-block seamounts, rather than the ~450 m found in basinal sections like Monte Acuto and Frontale (Alvarez, 1989; Cresta, 1989, p. 23-25).

2. METHODS

Bulk carbonate sample powders were extracted using a dental drill with a tungsten-carbide drill bit. In between drilling of different samples, the drill and drill bit were carefully cleaned with pressured air, ethanol and ultrapure 18.2 MΩ.cm water to avoid cross-contamination. Drilling was carried out using a drill bit of 0.5 mm in order to prevent sparry calcite cement from visible calcite veins- yielding a different isotopic signature, to mix with the limestone powders. Furthermore, sparry, calcite-cemented veins were separately sampled as well.

2.1 $^{87}Sr/^{86}Sr$

For Sr isotopic analysis of the carbonates, 100 mg of sample powder was accurately weighed in pre-cleaned Teflon® beakers. Next, 5 mL of 1M HCl was added to dissolve the samples. Along with the samples, one NIST SRM 987 $SrCO_3$ standard (National Institute for Standards and Technology, USA), several procedure blanks and sample duplicates were dissolved as well. Sample solutions appeared clear after dissolution with almost no visible residue. However, to fully eliminate any possible contribution from radiogenic ^{87}Sr leached from clay fractions in following steps involving concentrated strong acid attack, the solutions were centrifuged. After centrifugation, clear supernatant solutions were pipetted off and transferred to clean Teflon® vials. Next, the solutions were evaporated to near-dryness on a hotplate at 70°C and redissolved in 2mL of 7 M HNO_3. In addition, two samples (MMA-1tris and MMA-20tris) were subjected to a different dissolution procedure by adding 2 mL of 7 M HNO_3 instead of 5 mL of 1 M HCl. This was done in order to evaluate the influence of the use of highly concentrated acids (such as concentrated nitric acid) throughout the extraction procedure on the possible leaching of radiogenic Sr from the remaining clay fraction in the carbonate powders. Also, two international (silicate) rock reference standards (the basalt BE-N and micro gabbro PM-S obtained from the

Centre de Recherches Petrographiques et Géochimiques) were prepared following a different digestion protocol: 100 mg of sample powder was accurately weighed in clean Teflon® beakers and digested by addition and subsequent evaporation of 1) HF:HNO_3 (in a ratio of 2:4, 14 M HNO3 and 28M HF), (2) *Aqua regia*, (3) 14 M HNO_3 (4) 14 M HNO_3. Finally, the sample was redissolved in 7 M HNO_3.

The Sr was extracted using pre-packed BioRad columns, filled with 400 µL of the commercially available strontium-specific extraction chromatographic resin Sr spec™, and following an optimized procedure of De Muynck et al. (2009). $^{87}Sr/^{86}Sr$ ratios were subsequently measured using a Neptune multi-collector ICP-mass spectrometry (MC-ICP-MS) instrument at the Department of Chemistry at Ghent University. All samples were run in a sample-standard bracketing sequence with a 100 µg/L Sr isotopic standard solution of NIST SRM 987 $SrCO_3$. The Sr content in the samples and the standard was matched within ±10% to avoid any effect from the analyte content on the extent of instrumental mass discrimination. After every run, the sample introduction system was rinsed thoroughly with 2% HNO_3 to minimize memory effects. The results were mathematically corrected for mass bias using internal normalization to $^{86}Sr/^{88}Sr=0.1194$ by the exponential fractionation law.. The intensities obtained for $^{82}Kr^+$, $^{83}Kr^+$, and $^{85}Rb^+$ were used to correct for the Kr interferences on the m/z ratios of 84 and 86, and for the Rb interference on the m/z ratio of 87. The mean, long-term $^{87}Sr/^{86}Sr$ ratio obtained for NIST SRM 987 $SrCO_3$ was 0.710287 ± 0.000024 (2s.e., with N = 44). This is in full agreement with the accepted $^{87}Sr/^{86}Sr$ ratio of 0.710248 ±0.000011 (2s.d.) for this reference material (Thirlwall, 1991).

2.2 Carbon and oxygen isotope ratios

Carbon and oxygen isotope ratios were measured both with a Kiel-III-device coupled to a Thermo Delta plus XL isotope ratio mass spectrometer, and a a NuCarb automated carbonate preparation device coupled to a Nu Perspective Isotope Ratio Mass Spectrometer. Small quantities of carbonate powder were reacted with H_3PO_4 at a temperature of 75°C and the CO_2 generated was cryotrapped. Every set of six samples was bracketed by an international calcite standard (NBS-19 with $\delta^{18}O$ = -2.20 ± 0.01, $\delta^{13}C$ =+1.95 ± 0.02, or the NCM with $\delta^{18}O$ = -1.9 and $\delta^{13}C$= +2.09). Moreover, every sample was analysed three or four times on different measurement days. Carbon and oxygen isotopic results are reported on a per mil (‰) basis relative to the Vienna Pee Dee Belemnite (VPDB) standard. External analytical precision yielded values better than ± 0.015 ‰ for $\delta^{13}C$ and ±0.033‰ for $\delta^{18}O$ based on replicate analysis of the international calcite standards NBS-19 (US Geological Survey-USGS) and the in-house NCM (Cararra Marble, Nu instruments). Precision is reported as 1-sigma standard deviation.

3. RESULTS

3.1 Strontium, oxygen and carbon isotopic results

3.3.1 $^{87}Sr/^{86}Sr$

$^{87}Sr/^{86}Sr$ ratios vary between 0.70733 and 0.70758 (Tables 1, 2). The Sr isotopic trend accurately follows the McArthur seawater reference curve for the inferred stratigraphic interval (Late Berriasian ~141 Ma to Late Barremian ~127 Ma), but individual Sr isotope ratios are offset by +0.00007 to +0.0001 (Fig. 3). The $^{87}Sr/^{86}Sr$ of the calcite veins is much higher than the values of their host rock, yielding values between 0.70762-0.70777.

3.3.2 $\delta^{13}C$

Carbon isotope ratios cluster around plateau values of ~1.5‰ in the Berriasian to Early Valangian (Table 1, Fig.4). In The Mid-Valangian, $\delta^{13}C$ values rise rapidly to ~3‰ This positive C-isotopic of 1-1.5‰ excursion starts in the Valanginian *campylotoxus* ammonite zone, reaches peak values in the *verrucosum* zone and ends in the Hauterivian *radiatus* zone, corresponding to polarity chrons CM12–CM9 (Channell et al. 1993; Hennig et al. 1999; Weissert and Erba, 2004). Furthermore, this carbon isotopic excursion correlates with the well-defined Weissert Event, which is characterized by a positive $\delta^{13}C$ excursion of about 1 to 2‰ in marine carbonates. (Weissert and Erba, 2004), the first of four positive excursions recorded in the Cretaceous carbon isotopic record. In the Hauterivian, the $\delta^{13}C$ isotopic signature falls back to a background value of approximately ~2‰. Furthermore, carbon isotopic values in calcite veins reflect values of their host rock, suggesting they were buffered by the host rock during deposition of secondary calcite.

3.3.3 $\delta^{18}O$

Oxygen isotope ratio values range between -2.25‰ and -1.5‰ (Table 1). Compared to palaeogeographically comparable, selected sections from the Southern Alps (Weissert et al., 1985; Weissert and Channell, 1989), the oxygen values are depleted by approximately -1‰. On the other hand, oxygen isotope ratio values of the calcite veins document significant enrichment in the heavy ^{18}O and mostly yield positive $\delta^{18}O$ values, ranging between -0.65 to 2.44 ‰.

3.3.4 $^{87}Sr/^{86}Sr$, $\delta^{18}O$, $\delta^{13}C$ composite record

A composite strontium, carbon and oxygen isotope ratio record from Middle Berriasian to Late Barremian is presented in Fig. 4. Although broad and not very sharply bounded in our section, we can pinpoint the Mid-Valanginian positive excursion in the carbon isotopic record, identified as the Weissert Event, which correlates with a small (+0.0001), but resolvable positive spike in the $^{87}Sr/^{86}Sr$ curve. This excursion is very brief (~1 Ma) . In addition, the oxygen isotopic data yield a positive excursion with peak values corresponding exactly with the Sr spike. In the composite diagram, it can be seen that peak value of the carbon excursion, which covers approximately 5 Ma, is delayed with respect to the oxygen and Sr isotopic signal, which, in addition, cover a much smaller interval of time.

4. DISCUSSSION

4.1 Reliability of the $^{87}Sr/^{86}Sr$, $\delta^{13}C$ and $\delta^{18}O$ values

Before interpreting the isotopic records, it is important to assess whether the primary seawater isotopic values have been altered during post-depositional diagenetic processes and/or sample pre-treatment.

4.1.1 Oxygen isotope ratios

The process of recrystallization-dissolution will cause the $\delta^{18}O$ and the $\delta^{13}C$ of the carbonate to reequilibrate with the dissolved bicarbonate and the oxygen of the pore water. The Oxygen isotope ratios are most easily affected by diagenetic alteration. This is not solely because of a strong temperature-dependent fractionation, driving the $\delta^{18}O$ toward lower values as *in situ* temperature increases with sample depth in the sediment column (Matter et al., 1975; Schrag et al., 1995; Edgar et al., 2013). The lack of a "buffering" potential for oxygen during fluid-rock interaction is also due to huge amount of oxygen in water compared to the amount of dissolved carbonate in solution, and the relatively fast isotopic re-equilibration of oxygen in bicarbonate with oxygen in water.

4.1.2 Carbon isotope ratios

Compared to $\delta^{18}O$, the carbon isotope ratio values in carbonate rocks are less affected by diagenetic alteration. There is no (significant) temperature-dependent fractionation, and the $\delta^{13}C$ value is only measurably affected when recrystallization and cementation occur in the presence of pore water bicarbonate in which the $\delta^{13}C$ has been altered due to the addition of ^{12}C-enriched CO_2 derived from the oxidation of organic matter and microbial activity (Marshall, 1992; Maliva et al., 1995; Maliva and Dickson, 1997; Madhavaraju et al., 2013). Also, because the carbonate contains considerably more carbon than the pore waters, the $\delta^{13}C$

value of the recrystallized carbonates will be buffered by the host limestone and remain relatively unaltered. Indeed, excellent agreement between our data and the established $\delta^{13}C$ reference curves (Fig.4; Weissert and Erba, 2004; Sprovieri et al., 2006) from the Palaeo-Tethys indicates that the $\delta^{13}C$ value of the carbonate was not altered by the contribution of carbon from a secondary source.

4.1.3 Strontium Isotope ratios

Several processes may account for the elevated $^{87}Sr/^{86}Sr$ with respect to the seawater reference curve. In the following paragraph, these processes are discussed in light of diagenetic modifications, analytical bias and sample contamination.

As a first possible explanation, if the modified $^{87}Sr/^{86}Sr$ ratios were derived from pressure solution deeper in the stratigraphic column or expulsion of fluids derived from structurally lower formations, we would expect a shift to more negative $^{87}Sr/^{86}Sr$ ratios, based on the Sr seawater reference curve (McArthur et al., 2001), (Fig. 1). On the other hand, deep-burial diagenesis or hydrothermal fluid circulation of deep brines would shift the $^{87}Sr/^{86}Sr$ towards higher values, as deep brines usually acquire an excess of ^{87}Sr from interactions with clays or other silicate minerals, imparting this signature into late cements (Veizer, 1989). However, deep burial diagenesis would significantly shift the $\delta^{18}O$ value to more negative values, which is not consistent with our observations.

A second possible source of ^{87}Sr that could have offset the $^{87}Sr/^{86}Sr$ by +0.0001 is the presence of abundant, parallel calcite veins, which yield $^{87}Sr/^{86}Sr$ +0.0001-0.0002 higher compared the host Maiolica carbonate. However, the calcite-cemented veins yield positive $\delta^{18}O$ values. If sub-mm calcite cemented veins had been accidentally sampled during micro-drilling and

contaminated the carbonate powders, this would cause a measurable shift towards higher (more positive) $\delta^{18}O$ ratios of the bulk as well. This is not consistent with our data, which indicate that oxygen isotope ratios, if altered by diagenetic processes, would have shifted to slightly more positive values. Also, although one calcite vein contains an elevated Sr content compared to the host rock (Table1; PRE-3C), in other samples (FRO485C, FRO562.5C, MMA11.1, Table 1) concentrations are not much higher than the bulk rock from which the veins were sampled. In significantly higher concentration of Sr is required to affect the 87Sr/86Sr values of the bulk. In addition, the $^{87}Sr/^{86}Sr$ signature in other samples whit co-exisiting analysed veins (set for sample FROM485, FRO562.5, PRE-3) do not show spikes in the reconstructed $^{87}Sr/^{86}Sr$ record for the Maiolica., contamination from calcite veins requires this secondary calcite to represent a volumetrically significant component, which is not consistent with our observations.

A third possible candidate source for the observed increase in radiogenic Sr in the set of samples investigated may arise during the sample preparation and digestion procedure. Whole-rock carbonates may contain a negligible to large non-carbonate fraction, consisting of clay and/or organic matter. Given the fact that Sr^{2+} is relatively strongly adsorbed to phyllosilicates and organic matter, the presence of small amounts of non-carbonate fraction in a sample can increase the apparent $^{87}Sr/^{86}Sr$ values of carbonates (Burke et al., 1982), as clay minerals are enriched in radiogenic Sr. During sample dissolution dilute (1 M) hydrochloric acid was used to minimize the effect from any remaining clay/organic matter. Also, experiments with sample treatment procedures involving strong acid attack (see METHODS section) were evaluated by dissolving some of the samples with 7 M HNO_3 instead of dilute HCl. These samples yield $^{87}Sr/^{86}Sr$ ratios that are nearly-identical to those for samples leached with dilute HCl. Lastly, in all of the limestone samples analysed, very little or no clay or organic residue was observed, rendering Sr contamination from non-carbonate sources rather unlikely.

Renz and Habicht (1985) stated that the soft, unconsolidated pelagic sediments of the Blake–Bahama Formation, cored at DSDP Site 534A in the western central Atlantic, form an equivalent to the carbonate Maiolica facies in the Tethys (Bernoulli 1972, 2004). Similar to the Blake Bahama Fm, the Maiolica limestones must have originated from soft, coccolith ooze. At the sea floor, newly deposited calcareous ooze such as the Maiolica pelagic coccolith deposits has an estimated porosity around 70% (Matter et al., 1975), with interstitial pore water representing the chief component. In the Maiolica, the initially very high porosity was reduced to zero during burial, either by (1) mechanical compaction and/or by (2) pore filling cementation via pressure solution. Both are linked to the presence/absence of diagenetic fluid pathways, and the stress caused by the load of the overburden during progressive burial. During constant burial, porosity declines as a consequence of the load of the increasing overburden. Furthermore, during pressure solution and subsequent pore-filling cementation, interstitial pore waters will chemically reequilibrate with the surrounding carbonaceous ooze.

According to DePaolo and Finger (1991), recrystallization of soft, pelagic oozes should not substantially modify the $^{87}Sr/^{86}Sr$ ratio of the sediment. This presumption arises from the fact that during burial and lithification of calcareous ooze, diagenetic calcite is considered to be obtained from local (pressure) dissolution-recrystallization (Jenkyns et al., 1995). As a result, dissolution will deliver Sr to the pore fluids with an isotopic composition reflecting that of the dissolving carbonate. Subsequent reprecipitation will then precipitate calcite that has the same Sr isotope ratio as the pore fluid dissolved Sr. If dissolution-precipitation were the only diagenetic process involved, the pore fluids and the carbonate would yield the same isotope ratio at all depths, because the solid contains about 20 times more Sr than the pore fluid, buffering the isotopic ratio of the seawater it was deposited from (Fantle and DePaolo, 2006).

However, an important matter to take into account is that high-porosity sediments such as calcareous pelagic oozes are still in open, diffusive communication with the overlying seawater (and porous sediment). Diffusional migration in pore waters is caused by differences in concentration that develop between both sides of the sediment-water column interface (Lerman, 1978). Consequently, diffusion of aqueous Sr in the pore fluid will compete with the dissolution-precipitation process, homogenizing pore fluid concentrations and isotope ratios throughout the sediment column (Fantle and DePaolo, 2006).

Because the partition coefficient $D^{Sr}_{calcite} < 1$, the dissolution-reprecipitation of carbonates will result in a net increase in Sr concentration in the pore waters (Baker et al, 1982). During progressive burial and lithification, the Sr concentration in the pore waters will thus increase with depth. Gieskes et al. (1986) emphasized that the peak in Sr concentrations is associated with carbonate recrystallization reactions in the vicinity of the ooze-chalk transition, which represents a diagenetic front in the sediment column. So, because the secular trend in Sr isotope ratios throughout the Maiolica timeframe is one of constant increase (McArthur et al., 2001), and because the down-gradient rate of Sr diffusion exceeds the rate of *in situ* recrystallization, the water above the Sr concentration maximum is depleted, and that below enriched, in ^{87}Sr. The *in situ* diagenetically precipitated carbonates then inherit this pore water Sr and shift the bulk-rock isotopic composition toward that of the ambient pore waters.

Because the secular trend in Sr isotope ratios throughout the Maiolica timeframe is one of constant increase, before declining in the Mid-Barremmian, the $^{87}Sr/^{86}Sr$ ratios of the Maiolica carbonates may have systematically displaced from that of the seawater in which it was deposited towards more radiogenic values. This is in accordance with modelling studies from

550 Richter and De Paolo (1987), who developed a numerical model for the diagenetic exchange of
551 Sr between chalks and their pore fluids during sedimentation and compaction in order to assess
552 the accuracy with which the Sr isotope record in the carbonate sediment reflects that of
553 seawater. Based on modelling studies, the authors postulate that for sediments older than 5 Ma
554 the $^{87}Sr/^{86}Sr$ ratio of the carbonate is systematically displaced from that of the seawater in which
555 it was deposited, with a maximum difference of +0.00005.
556 Considering this as an explanation for elevated $^{87}Sr/^{86}Sr$ compared to the global marine
557 reference curve, diffusional migration and pore water exchange should also have affected the
558 Sr isotopic signature in the upper part of the Maiolica succession, at least plateauing or ideally
559 decreasing the $^{87}Sr/^{86}Sr$ at the respective stratigraphic interval. Our data show that the offset
560 towards higher $^{87}Sr/^{86}Sr$ indeed seems to reach a plateau in the upper part of the section,
561 although a decrease is not observed. Therefore it seems unlikely that diffusional migration was
562 the only process affecting the $^{87}Sr/^{86}Sr$ of the Maiolica. During compaction, release of
563 interlayer water from clays (in the small silicate fraction)-carrying a radiogenic $^{87}Sr/^{86}Sr$
564 signature, into to the pore water may have slightly offset the Sr isotopic composition if the pore
565 water.
566
567 Both C and O isotopic data are in agreement with the hypothesis of diffusional migration and
568 pore water exchange. Carbon isotope ratios remain unchanged as they are buffered by the
569 bicarbonate dissolved from the carbonate host. Contrary, although relative variations in the
570 oxygen isotopic record have remained unchanged, all values seem offset by approximately -1
571 ‰. Considering the geothermal gradient and the strong temperature-dependent fractionation of
572 the oxygen isotopic system, this -1‰ shift to a more negative $\delta^{18}O$ value is a result of the
573 roughly 5°C warmer temperatures at a burial depth of 50-250m, the depth at which gravitational
574 compaction and dissolution-precipitation will dominate the lithification process of calcareous

oozes (Larsen and Chilingar, 1983Consequently, our Sr, O and C isotopic data support the hypothesis that the offset in $^{87}Sr/^{86}Sr$ results from incorporation of excess ^{87}Sr through isotopic reequilibration of carbonate with interstitial pore waters during progressive lithification of the calcareous ooze during diagenesis at slightly elevated temperatures.

4.2 The Weissert Event: constraints from Sr, O and C isotopic data

The Weissert Event has been recognized in Valanginian pelagic sediments of all the major oceans, including the Pacific (Weissert and Erba, 2004; Bartolini, 2003) and in shallow-water carbonate successions of the northern Tethys (Föllmi et al. 1994) and in fossil wood records (Gröcke et al. 2003). The Valanginian positive carbon isotope excursion thus seems to be of global extent and may serve as a useful stratigraphic marker (Weissert et al., 2008).

The Weissert Event is the first of a series of Cretaceous excursions in the global $\delta^{13}C$ isotopic record.

The onset of the excursion in the Mid-Valanginian coincides with the onset of increased volcanic activity. This volcanism was essentially subaerial and localized in the Paranà–Etendeka province. Weissert and Erba (2004) suggested that the increase in atmospheric CO_2 resulting from increased subaerial volcanism may have caused accelerated weathering and hydrological cycling and thus indirect increased fertilization in coastal environments. Subsequent increased bioproductivity caused a drawdown of ^{12}C from the DIC reservoir in the oceans, increasing the $\delta^{13}C$ of the seawater, as recorded in authigenic marine carbonates.

Interestingly, there is isotopic and biotic evidence for a Valanginian cooling event coinciding with the time of the positive carbon isotopic excursion, based on (1) increased $\delta^{18}O$ values in

marine carbonates, (2) the increase of boreal nannofossils in Romania (Melinte and Mutterlose, 2001) and (3) the occurrence of the nanofossil *Kokia borealis* in the equatorial Pacific (Weissert and Erba, 2004). Our data also show a peak in positive $\delta^{18}O$ values in the Maiolica-at the base of the Valanginian carbon excursion (Fig. 4). This peak coincides with a shift in the Sr seawater curve to higher $^{87}Sr/^{86}Sr$. Interestingly, the $^{87}Sr/^{86}Sr$ peak we observe at the Weissert Event is not resolved by the Global Sr marine reference curve. However, the Sr marine reference curve assumes a global nature of the Sr-isotope signal. This assumption is true for modern major ocean basins that are well-connected with each other, yielding a relatively fast mixing time of 1500 years. However, it may not be an entirely valid assumption for past time-periods. Basins (such as the Umbria-Marche basin during the Early Cretaceous) might be relatively constricted, and if the size of the fluxes becomes much larger (with respect to the reservoir), the residence time of Sr may become shorter. This may play a role in the Sr excursions during extreme climate events, such as the Weissert Event.

Since elevated $^{87}Sr/^{86}Sr$ ratios in past oceanic seawater are a proxy for increased continental runoff, it can be regarded as a tool for tracing the causal connection between cycles of weathering and climatic perturbation, and the palaeobiotic response to these environmental changes. Although it must be emphasized that the climate-driven approach to global weathering (Ruddiman et al., 1997) is controversial and beyond the scope of this paper, some interesting interpretations can be offered. The source of the weathering/climate connection is the atmospheric CO_2. It is thought that high CO_2 conditions in the atmosphere induce greater rainfall and temperatures, increasing the rate of continental chemical weathering, enhancing the flux of continental-derived (radiogenic) Sr to the oceans and increasing their $^{87}Sr/^{86}Sr$ (Ruddiman et al., 1997). In its turn, the process of weathering consumes the atmospheric CO_2, exerting a negative feedback mechanism which triggers global cooling. In addition, increased

625 continental runoff induces indirect fertilisation of the oceans, stimulating bioproductivity. This
626 results in a drawdown of light ^{12}C from the oceans, and causes a positive shift in the $\delta^{13}C$ record.
627 Elevated CO_2 levels may be explained by increased volcanic activity in the Paranà-Etendeka
628 province during the Valanginian Weissert Event (Weissert and Erba, 2004). This hypothesis
629 fits with elevated $^{87}Sr/^{86}Sr$, $\delta^{18}O$ and $\delta^{13}C$ values throughout the Valanginian.
630
631 An interesting observation is that the peak in the positive $\delta^{13}C$ excursion in the Valanginian
632 post-dates both the strontium and oxygen isotopic shifts (Fig. 2) This contrasts with the
633 observations of Weissert and Erba (2004), who state that the Valanginian cooling episode
634 occurs within the *verrucosum* ammonite zone and should coincide with the heaviest $\delta^{13}C$
635 values. Considering our good biostratigraphic and magnetostratigraphic age control, the
636 'delayed' response of the carbon isotopic signal is likely a diagenetic artefact inherent to the Sr
637 and O isotopic signals rather than a primary feature. In fact, it would seem that it is not the
638 carbon signal that is delayed, but the Sr and O signatures that are shifted due to the diffusive
639 communication of Sr from the pore waters in the overlying sediments and the seawater column
640 into pore water during recrystallization-precipitation of the calcareous ooze. This process will
641 only affect the $\delta^{18}O$ and $^{87}Sr/^{86}Sr$ values, biasing their true stratigraphic, depositional age
642 towards older ages, while the $\delta^{13}C$ system remains largely unaffected by this process.
643
644 Alternatively the positive spike in $\delta^{18}O$ and $^{87}Sr/^{86}Sr$ at the onset of the Weissert event can be
645 explained by sample MMA11.2 being compromised by the vein calcite at the same stratigraphic
646 level which is enriched in ^{18}O and ^{87}Sr. If one assumes the original geochemical data for
647 MMA11.2 to be the average of MMA12 and MMA10, a 60:40 mix of bulk rock and vein calcite
648 will generate the observed $\delta^{18}O$ and $^{87}Sr/^{86}Sr$ spikes. This admixture may not be in the form of
649 sparry calcite but may just be diffuse microcrystalline calcite formed within the rock matrix at

650 the same time as the vein. However, we have sampled veins from other bulk rock samples (e.g.
651 FRO 485.C, FRO 562.5C, PRE-3.C, Table 1). If we compare with the values for the host rock,
652 the $^{87}Sr/^{86}Sr$ signature of the bulk is not biased towards more positive $\delta^{8}O$ and higher $^{87}Sr/^{86}Sr$,
653 as is the case for sample MMA11. Therefore we believe this positive excursion in our $^{87}Sr/^{86}Sr$
654 record is a primary feature.
655

656 ## 5. CONCLUSION

657 This study provides a composite record of $^{87}Sr/^{86}Sr$, $\delta^{18}O$ and $\delta^{13}C$ for three sections in the
658 Tethyan Early Cretaceous Maiolica sequence, carefully tied to a magnetostratigraphically and
659 biostratigraphically calibrated timescale. The Sr isotope ratio record follows the general trend
660 of the Global Strontium isotope ratio seawater reference curve, though individual $^{87}Sr/^{86}Sr$
661 ratios are systematically offset by +0.00007. We conclude that this offset results from
662 incorporation of excess ^{87}Sr through isotopic re-equilibration with interstitial pore waters during
663 progressive compaction and lithification of the principal calcareous ooze, with a small
664 contribution from calcite micro-veins.
665

666 Furthermore, the (pristine) carbon isotope seawater record allows identification of the Mid-
667 Valanginian Weissert event, characterized by a positive excursion in the $\delta^{13}C$ and the $\delta^{18}O$
668 record. In our record, the Weissert event correlates with a positive peak (+0.0001) in $^{87}Sr/^{86}Sr$.
669 Both the Sr and O isotopic peaks pre-date the maximum peak in the $\delta^{13}C$ excursion. If we
670 assume the excursion in the $\delta^{18}O$ and $^{87}Sr/^{86}Sr$ to reflect the oceanic conditions,this delay is
671 likely a diagenetic artefact and further strengthens the hypothesis of diffusive communication
672 of Sr with overlying water column during lithification of the calcareous ooze.
673

674 The theory of diffusive communication versus dissolution-reprecipitation elegantly explains
675 our systematic offset in Sr isotopic data from the seawater reference curve and the shift in the
676 peak values of Sr and O isotopic excursions with respect to the $\delta^{13}C$ record in the Mid-
677 Valanginian Weissert Event. In addition, this study highlights the importance of assessing the
678 degree of diagenetic alteration using chemostratigraphic tools. In this context, it must be noted
679 that the marine Sr reference curve (McArthur et al., 2001) is constructed based on measurement
680 of (unaltered) low-Mg calcite shells instead of bulk carbonate rock. The reliability of the records
681 therefore depends on how well unaltered forams/bivalves can be identified and separated.
682 Richter and DePaolo (1987) stated that separates consisting of varying proportions of altered
683 and unaltered forams may bias the data set, generating a source of noise that may hide the
684 subtler aspects of $^{87}Sr/^{86}Sr$ variation with time in the ocean. On the other hand, it is expected
685 that measuring the $^{87}Sr/^{S6}Sr$ of bulk carbonate data may lead to Sr isotopic signatures slightly
686 deviating from the reference curve. However, contrary to the use of calcite shells, bulk
687 carbonate data may generate less noisy data because of more consistent sampling. In summary,
688 applying chemostratigraphy as a correlation tool must always be assessed in the light of the
689 diagenetic processes involved, as the Sr isotopic curve of palaeoceans cannot be constrained
690 better than that dictated by diagenetic considerations (Veizer, 1989).
691
692
693
694
695
696
697
698

6. ACKNOWLEDGEMENTS

Joke Belza acknowledges the Research Foundation Flanders (FWO) for its support in funding a PhD Fellowship. Alessandro Montanari and the Geological Observatory of Coldigioco provided logistical support during fieldwork. We thank John McArthur for sharing his $^{87}Sr/^{86}Sr$ data in the early phases of this study. We thank Jim Channell for orientation data on his drill holes in the MMA section, and Bill Lowrie for orientation data on drill holes at FRO.

7. REFERENCES

Alvarez, W., 1989, Evolution of the Monte Nerone seamount in the Umbria-Marche Apennines: 1. Jurassic-Tertiary stratigraphy: Societá Geologica Italiana, Bollettino, v. 108, p. 3-21.

Alvarez, W., 2009, The historical record in the Scaglia limestone at Gubbio: magnetic reversals and the Cretaceous-Tertiary mass extinction: Sedimentology, v. 56, no. 1, p. 137-148.

Alvarez, W., Arthur, M. A., Fischer, A. G., Lowrie, W., Napoleone, G., Premoli Silva, I., and Roggenthen, W. M., 1977, Upper Cretaceous-Paleocene magnetic stratigraphy at Gubbio, Italy: V. Type section for the Late Cretaceous-Paleocene geomagnetic reversal time scale: Geological Society of America Bulletin, v. 88, p. 383-389.

Baker, P. A., Gieskes, J. M., and Elderfield, H., 1982, Diagenesis of carbonates in deep-sea sediments--evidence from Sr/Ca ratios and interstitial dissolved Sr^{2+} data: Journal of Sedimentary Petrology, v. 52, no. 71-82.

Bartolini, A., 2003, Cretaceous radiolarian biochronology and carbon isotope stratigraphy of ODP Site 1149 (Northwestern Pacific, Nadezhda Basin): Proceedings of the Ocean Drilling Program - Scientific Results, v. 185.

Bernoulli, D., 1972, North Atlantic and Mediterranean Mesozoic facies. : Initial Reports of the Deep Sea Drilling Project v. 11, p. 801-871.

Bernoulli, D., Gasperini, L., Bonatti, E., and Stille, P., 2004, Dolomite formation in Pelagic limestone and diatomite, Romanche Fracture Zone, equatorial Atlantic (Articolo in rivista): Journal of Sedimentary Research, v. 74, no. 6, p. 924-932.

Burke, W. A., Denison, R. E., Hetherington, E. A., Koepnik, R. B., Nelson, H. F., and Otto, J. B., 1982, Variation of seawater $^{87}Sr/^{86}Sr$ throughout Phanerozoic time: Geology, v. 10, p. 516-519.

Cecca, F., 1995, Late Valanginian ammonites from Monte Catria (Umbria-Marche Apennines, Italy): Memorie Descrittive della Carta Geologica d'Italia, v. 51, p. 47-57.

Cecca, F., Marini, A., Pallini, G., Baudin, F., and Begouen, V., 1994, A guide-level of the uppermost Hauterivian (Lower Cretaceous) in the pelagic succession of Umbria-Marche Apennines (Central Italy): The Faraoni Level: Rivista Italiana di Paleontologia e Stratigraphia, v. 99, no. 4, p. 551-568.

Channell, J. E. T., Cecca, F., and Erba, E., 1995, Correlations of Hauterivian and Barremian (Early Cretaceous) stage boundaries to polarity chrons: Earth and Planetary Science Letters, v. 134, p. 125-140.

Channell, J. E. T., Erba, E., and Lini, A., 1993, Magnetostratigraphic calibration of the Late Valanginian carbon isotope event in pelagic limestones from Northern Italy and Switzerland: Earth and Planetary Science Letters, v. 118, no. 1–4, p. 145-166.

Coccioni, R., Baudin, F., Cecca, F., Chiari, M., Galeotti, S., Gardin, S., and Salvini, G., 1998, Integrated stratigraphic, palaeontological, and geochemical analysis of the uppermost Hauterivian Faraoni Level in the Fiume Bosso Section, Umbria-Marche Apennines, Italy: Cretaceous Research, v. 19, no. 1, p. 1-23.

Coccioni, R., and Montanari, A., 2018, Thirty years of Lower Cretaceous to Miocene integrated stratigraphy in the Umbria-Marche Apennines, central Italy: this volume.

Cresta, S., Monechi, S., Parisi, G., Baldanza, A., and Reale, V., 1989, Stratigrafia del Mesozoico e Cenozoico nell'area Umbro-Marchigiana/Mesozoic-Cenozoic stratigraphy in the Umbria-Marche area [in Italian and English]: Memorie Descrittive della Carta Geologica d'Italia, v. 39, no. 185.

De Muynck, D., Huelga-Suarez, G., Van Heghe, L., Degryse, P., and Vanhaecke, F., 2009, Systematic evaluation of a strontium-specific extraction chromatographic resin for obtaining a purified Sr fraction with quantitative recovery from complex and Ca-rich matrices: Journal of Analytical Atomic Spectrometry, v. 24, no. 11, p. 1498-1510.

DePaolo, D. J., and Finger, K. L., 1991, High-resolution strontium-isotope stratigraphy and biostratigraphy of the Miocene-Monterey-Formation, central California: Geological Society of America Bulletin, v. 103 no. 1, p. 112-124.

Edgar, K. M., Pälike, H., and Wilson, P. A., 2013, Testing the impact of diagenesis on the δ18O and δ13C of benthic foraminiferal calcite from a sediment burial depth transect in the equatorial Pacific: Paleoceanography, v. 28, no. 3, p. 468-480.

Fantle, M. S., and DePaolo, D. J., 2006, Sr isotopes and pore fluid chemistry in carbonate sediment of the Ontong Java Plateau: Calcite recrystallization rates and evidence for a rapid rise in seawater Mg over the last 10 million years: Geochimica et Cosmochimica Acta, v. 70, no. 15, p. 3883-3904.

Faraoni, P., Flore, D., Marini, A., Pallini, G., and Pezzoni, N., 1997, Valanginian and early Hauterivian ammonite successions in the Monte Catria group (Central Apennines) and in the Lessini Mts (Southern Alps), Italy: Palaeopelagos, v. 7, p. 59-100.

Faure, G., and Powell, J. L., 1972, Strontium Isotope Geology, New York, Springer-Verlag, 188 p.:

Föllmi, K. B., Weissert, H., Bisping, M., and Funk, H., 1994, Phosphogenesis, carbon-isotope stratigraphy and carbonate platform evolution along the northern Tethyan margin.: Geological Society of America Bulletin, v. 106, p. 729-746.

Frijia, G., and Parente, M., 2008, Strontium isotope stratigraphy in the upper Cenomanian shallow-water carbonates of the southern Apennines: Short-term perturbations of marine 87Sr/86Sr during the oceanic anoxic event 2: Palaeogeography, Palaeoclimatology, Palaeoecology, v. 261, no. 1–2, p. 15-29.

Gieskes, J. M., Elderfield, H., and Palmer, M. R., 1986, Strontium and its isotopic composition in interstitial waters of marine carbonate sediments: Earth and Planetary Science Letters, v. 77, no. 2, p. 229-235.

Grippo, A., Fischer, A. G., Hinnov, L. A., Herbert, T. D., and Premoli SilvaI., I., 2004, Cyclostratigraphy and chronology of the Albian stage (Piobbico core, Italy): Special Publication - Society for Sedimentary Geology, v. 81, p. 57-81.

Gröcke, D. R., Price, G. D., Baraboshkin, E., Mutterlose, J., and Ruffell, A. H., 2003, The Valanginian terrestrial carbon-isotope record: Geophysical Research Abstracts, v. 5

Grossman, E. L., 2012, Chapter 10 - Oxygen Isotope Stratigraphy, *in* Gradstein, F. M., Schmitz, J. G. O. D., and Ogg, G. M., eds., The Geologic Time Scale: Boston, Elsevier, p. 181-206.

Hennig, S., Weissert, H., and Bulot, L., 1999, C-isotope stratigraphy, a calibration tool between ammonite- and magnetostratigraphy: Geologica Carpathica, v. 50, p. 91-96.

Howarth, R. J., and Mcarthur, J. M., 1997a, Statistics For Strontium Isotope Stratigraphy: A Robust Lowess Fit to the Marine Sr-Isotope Curve For 0 to 206 Ma, With Look-Up Table For Derivation of Numeric Age: The Journal of Geology, v. 105, no. 4, p. 441-456.

Howarth, R. J., and McArthur, J. M., 1997b, Statistics for Strontium Isotope Stratigraphy: A Robust LOWESS Fit to the Marine Sr-Isotope Curve for 0 to 206 Ma, with Look-up Table for Derivation of Numeric Age: The Journal of Geology, v. 105, p. 441-456.

Jenkyns, H. C., Paull, K., Cummins, D. I., and Fullagar, P. D., 1995, Strontium-isotope stratigraphy of lower Cretaceous atoll carbonates in the mid Pacific Mountains: Proceedings of the Ocean Drilling Program - Scientific Results, v. 143, p. 89-97.

Larsen, G., and Chilingar, G. V., 1983, Diagenesis in Sediments and Sedimentary Rocks 2, Amsterdam, Elsevier Scientific.

Lowrie, W., and Alvarez, W., 1977, Upper Cretaceous-Paleocene magnetic stratigraphy at Gubbio, Italy: III. Upper Cretaceous magnetic stratigraphy: Geological Society of America Bulletin, v. 1977, p. 374-377.

Lowrie, W., and Alvarez, W., 1984, Lower Cretaceous magnetic stratigraphy in Umbrian pelagic limestone sections.: Earth and Planetary Science Letters, v. 71, p. 315-328.

Lowrie, W., Alvarez, W., Premoli Silva, I., and Monechi, S., 1980, Lower Cretaceous magnetic stratigraphy in Umbrian pelagic carbonate rocks: Geophysical Journal, v. 60, p. 263-281.

Madhavaraju, J., Lee, Y. I., and González–León, C. M., 2013, Diagenetic significance of carbon, oxygen and strontium isotopic compositions in the Aptian-Albian Mural Formation in Cerro Pimas area, northern Sonora, Mexico: Journal of Iberian Geology v. 39 no. 1, p. 73-88.

Maliva, R. G., and Dickson, J. A. D., 1997, Ulster white limestone formation (Upper Cretaceous)of Northern Ireland: effects of basalt loading on chalk diagenesis: Sedimentology v. 44, no. 105-112.

Maliva, R. G., Dickson, J. A. D., Smalley, P. C., and Oxtoby, N. H., 1995, Diagenesis of the Machar field (British North-Sea) chalk: evidence for decoupling of diagenesis in fractures and the host rock: Journal of Sedimentary Research v. 65, no. 105-111.

Marshall, J. D., 1992, Climatic and oceanographic isotopic signals from the carbonate rock record and their preservation: Geological Magazine, v. 129, no. 143-160.

Matter, A., Douglas, R. G., and Perch-Nielson, K., 1975, Fossil preservation, biochemistry, and diagenesis of pelagic carbonates from Shatsky Rise, northwest Pacific: Proceedings of the Ocean Drilling Program, Initial Reports, no. 32, p. 891-907.

McArthur, J. M., Howarth, R. J., and Bailey, T. R., 2001, Strontium Isotope Stratigraphy: LOWESS Version 3: Best Fit to the Marine Sr-Isotope Curve for 0–509 Ma and Accompanying Look-up Table for Deriving Numerical Age: The Journal of Geology, v. 109, p. 155–170.

McArthur, J. M., Howarth, R. J., and Shields, G. A., 2012, Chapter 7 - Strontium Isotope Stratigraphy, *in* Gradstein, F. M., Schmitz, J. G. O. D., and Ogg, G. M., eds., The Geologic Time Scale: Boston, Elsevier, p. 127-144.

Melinte, M., and Mutterlose, J., 2001, A Valanginian (Early Cretaceous) 'Boreal nannoplankton excursion' in sections from Romania: Marine Micropaleontology, v. 43, p. 1-25.

Montanari, A., and Koeberl, C., 2000, Impact stratigraphy: the Italian record, *in* Bhattacharji, S., Friedman, G. M., Neugebauer, H. J., and Seilacher, A., eds., Lecture Notes in Earth Sciences, Volume 93: Berlin, Springer Verlag, p. 364.

Palmer, M. R., and Edmond, J. M., 1989, The strontium isotope budget of the modern ocean: Earth and Planetary Science Letters, v. 92, no. 1, p. 11-26.

Renz, O., and Habicht, K., 1985, A correlation of the Tethyan Maiolica Formation of the Breggia section (southern Switzerland) with Early Cretaceous oozes of Site 534A, DSDP Leg 76 in the western Atlantic: Eclogae Geologicae Helvetiae, v. 78 no. 2 p. 383-431.

Richter, F. M., and DePaolo, D. J., 1987, Numerical models for diagenesis and the Neogene Sr isotopic evolution of seawater from DSDP Site 590B: Earth and Planetary Science Letters, v. 83, no. 1–4, p. 27-38.

Rohling, E. J., and Bigg, G. R., 1998, Paleosalinity and δ18O: A critical assessment: Journal of Geophysical Research: Oceans, v. 103, no. C1, p. 1307-1318.

Ruddiman, W. F., Kutzbach, J. E., and Prentice, C., 1997, Testing the climatic effects of orography and CO_2 with general circulation and biome models, *in* Ruddiman, W. F., ed., Tectonic uplift and climate change: New York, Plenum Press, p. 203-235.

Schrag, D. P., DePaolo, D. J., and Richter, F. M., 1995, Reconstructing past sea surface temperatures: Correcting for diagenesis of bulk marine carbonate: Geochimica et Cosmochimica Acta, v. 59, no. 11, p. 2265-2278.

Shackleton, N., 1967, Oxygen Isotope Analyses and Pleistocene Temperatures Re-assessed: Nature, v. 215, no. 5096, p. 15-17.

Sprovieri, M., Coccioni, R., Lirer, F., Pelosi, N., and Lozar, F., 2006, Orbital tuning of a Lower Cretaceous composite record (Maiolica Formation, central Italy): Paleoceanography, v. 21, no. 4, p. 19.

Sundquist, E. T., and Visser, K., 2003, 8.09 - The Geologic History of the Carbon Cycle, *in* Turekian, H. D. H. K., ed., Treatise on Geochemistry: Oxford, Pergamon, p. 425-472.

Thirlwall, M. F., 1991, Long-term reproducibility of multi-collector Sr and Nd isotope ratio analysis: Chemical Geology, v. 94, p. 85-104.

Veizer, J., 1989, Strontium Isotopes in Seawater through Time: Annual Review of Earth and Planetary Sciences, v. 17, no. 1, p. 141-167.

874 Veizer, J., Ala, D., Azmy, K., Bruckschen, P., Buhl, D., Bruhn, F., Carden, G. A. F., Diener, A., Ebneth, S.,
875 Godderis, Y., Jasper, T., Korte, C., Pawellek, F., Podlaha, O. G., and Strauss, H., 1999, $^{87}Sr/^{86}Sr$,
876 $\delta^{13}C$ and $\delta^{18}O$ evolution of Phanerozoic seawater: Chemical Geology, v. 161, no. 1-3, p. 59-88.
877 Veizer, J., Fritz, P., and Jones, B., 1986, Oxygen and carbon isotopic records of Paleozoic oceans:
878 Geochimica et Cosmochimica Acta, v. 50, p. 1679-1696.
879 Weissert, H., and Erba, E., 2004, Volcanism, CO_2 and palaeoclimate: a Late Jurassic–Early Cretaceous
880 carbon and oxygen isotope record: Journal of the Geological Society, v. 161, no. 4, p. 695-702.
881 Weissert, H., Joachimsky, M., and Sarnthein, M., 2008, Chemostratigraphy: Newsletters on
882 Stratigraphy, v. 42, no. 3, p. 145-179.
883 Weissert, H., McKenzie, J. A., and Channell, J. E. T., 1985, Natural variations in the carbon cycle during
884 the Early Cretaceous, *in* Sundquist, E. T., and Broeker, W. S., eds., The Carbon Cycle and
885 Atmospheric CO_2: Natural Variations Archean to Present Volume 32, American Geophysical
886 Union, p. 531-545.
887 Weissert, H. C., J.E.T. , 1989, Tethyan carbonate carbon isotope stratigraphy across the Jurassic-
888 Cretaceous boundary: an indicator of decelerated carbon cycling. : Paleoceanography, v. 4, p.
889 483-494.
890 Zeebe, R. E., and Wolf-Gladrow, D., 2001, CO_2 in seawater: Equilibrium, kinetics, isotopes, Amsterdam,
891 Elsevier, Elsevier Oceanography Series.

892

893

894 **FIGURE CAPTIONS**

895 Figure 1. Locality map for the sections sampled in this study: Frontale (FRO) Presale (PRE)
896 and Monte Acuto (MMA)

897

898 Figure 2. The upper Valanginian portion of the Maiolica exposed at the MMA section. The
899 section in this view extends about 40 m along the road, and the beds dip southwest, on the
900 southwest flank of the Monte Acuto-Monte Catria anticline; the center of the photo is at 43°
901 27.828'N, 12° 40.380'E.

902

903 Figure 3. Isotopic data and age calibration for the Maiolica of the Monte Acuto, Frontale and
904 Presale stratigraphic sections. GTS 2012 = Geologic Time Scale 2012 (Gradstein et al., 2012).
905 For details of the polarity zonation, see Ogg, 2012, GTS 2012, Table 5.2. For the Tethyan
906 ammonite zonation, see Ogg and Hinov, 2012, GTS 2012, p. 813

907

908 Figure 4. Composite curve $^{87}Sr/^{86}Sr$, $\delta^{18}O$ and $\delta^{13}C$ for the Monte Acuto stratigraphic section.

909 Samples are plotted with equal spacing.

910

911

Table 1

Table 1 $^{87}SR/^{86}SR$, SR CONTENT AND TABLE ISOTOPIC COMPOSITIONS FOR PRESALE, FRONTALE AND MONTE ACUTO SECTIONS

lithology	SECTION	**Sample ID**	**$^{87}Sr/^{86}Sr$**	**sd***	**SE†**	**RSD§**	**Sr (µg/g)**	**$\delta^{13}C$ (‰)#**	**$\delta^{18}O$ (‰)#**
bulk CaCO3	Presale	PRE-1	0.70746	0.00004	0.00001	0.011	235	2.06	-1.85
bulk CaCO3	Presale	PRE-2	0.70748	0.00005	0.00001	0.014	202	2.23	-1.99
bulk CaCO3	Presale	PRE-3	0.70751	0.00004	0.00001	0.012	190	1.99	-1.86
bulk CaCO3	Presale	PRE-4	0.70755	0.00003	0.00000	0.007	197	1.86	-2.25
bulk CaCO3	Presale	PRE-5	0.70751	0.00004	0.00001	0.013	199	2.03	-2.12
bulk CaCO3	Presale	PRE-6	0.70754	0.00004	0.00001	0.011	205	1.74	-2.25
bulk CaCO3	Presale	PRE-7	0.70756	0.00003	0.00001	0.009	222	1.87	-2.01
bulk CaCO3	Presale	PRE-8	0.70752	0.00004	0.00001	0.012	356	2.21	-1.91
bulk CaCO3	Presale	PRE-9	0.70753	0.00004	0.00001	0.012	231	2.60	-1.88
bulk CaCO3	Presale	PRE-10	0.70752	0.00005	0.00001	0.014	281	2.21	-1.93
calcite vein	Presale	PRE-3.C	0.70761	0.00003	0.00001	0.010	197	2.19	0.34
				0.00000					
bulk CaCO3	Frontale	FRO-470	0.70743	0.00004	0.00001	0.011	181	3.10	-1.74
bulk CaCO3	Frontale	FRO-485	0.70746	0.00004	0.00001	0.012	378	2.65	-1.43
bulk CaCO3	Frontale	FRO-502	0.70748	0.00004	0.00001	0.012	200	2.37	-1.55
bulk CaCO3	Frontale	FRO-510	0.70748	0.00005	0.00001	0.014	206	2.22	-1.52
bulk CaCO3	Frontale	FRO-521	0.70752	0.00003	0.00001	0.009	170	2.11	-1.63
bulk CaCO3	Frontale	FRO-530	0.70753	0.00004	0.00001	0.011	162	1.94	-1.81
bulk CaCO3	Frontale	FRO-540	0.70752	0.00004	0.00001	0.011	148	1.83	-1.87
bulk CaCO3	Frontale	FRO-567	0.70753	0.00005	0.00001	0.013	174	2.14	-1.41
bulk CaCO3	Frontale	FRO-550	0.70752	0.00004	0.00001	0.012	169	1.62	-1.86
bulk CaCO3	Frontale	FRO-560	0.70754	0.00004	0.00001	0.011	165	1.83	-1.47
bulk CaCO3	Frontale	FRO-561	0.70753	0.00004	0.00001	0.012	168	1.84	-1.39
bulk CaCO3	Frontale	FRO-562.5	0.70754	0.00005	0.00001	0.013	163	1.78	-1.49
bulk CaCO3	Frontale	FRO-563	0.70752	0.00004	0.00001	0.011	161	1.72	-1.56
bulk CaCO3	Frontale	FRO-565	0.70752	0.00004	0.00001	0.012	193	2.02	-1.21
bulk CaCO3	Frontale	FRO-566	0.70751	0.00004	0.00001	0.010	181	2.19	-1.25
bulk $CaCO_3$	Frontale	FRO-568	0.70756	0.00004	0.00001	0.012	182	2.19	-1.37
bulk $CaCO_3$	Frontale	FRO-569.5/2	0.70753	0.00005	0.00001	0.013	168	2.12	-1.68
bulk $CaCO_3$	Frontale	FRO-570	0.70749	0.00004	0.00001	0.011	166	2.01	-1.41
bulk $CaCO_3$	Frontale	FRO-571.6	0.70758	0.00004	0.00001	0.012	164	1.78	-1.29

bulk CaCO3	Frontale	FRO-580	0.70756	0.00004	0.00001	0.012	178	2.23	-1.55
bulk CaCO3	Frontale	FRO-594	0.70757	0.00005	0.00001	0.013	177	2.41	-1.26
bulk CaCO3	Frontale	FRO-597	0.70752	0.00004	0.00001	0.012	177	2.39	-1.36
				0.00000					
calcite vein	Frontale	FRO-562.5C	0.70777	0.00019	0.00003	0.054	n.a.	2.15	-0.65
calcite vein	Frontale	FRO-585.C	0.70765	0.00004	0.00001	0.011	148	2.62	2.44
				0.00000					
replicate	Frontale	PRE-1BIS	0.70748	0.00004	0.00001	0.011	225	n.a. **	n.a. **
replicate	Frontale	FRO-560BIS	0.70754	0.00004	0.00001	0.011	154	n.a.	n.a.
replicate	Frontale	FRO-566BIS	0.70751	0.00004	0.00001	0.011	n.a.	n.a.	n.a.
replicate	Frontale	FRO-594BIS	0.70750	0.00003	0.00001	0.008	153	n.a.	n.a.

lithology	sample type	**Sample ID**	**$^{87}Sr/^{86}Sr$**	**sd**	**SE†**	**RSD§**	**Sr (µg/g)**	**Reference value (GEoREM) $^{87}Sr/^{86}Sr$**	**Reference value (GEoREM) Sr (µg/g)**
micro-gabbro	Geostandard ††	PM-S	0.70461	0.00003	0.00001	0.009	241	0.704596	270 - 296 µg/g (compiled: 275 - 280 µg/g , 2 values)
basalt	Geostandard ††	BEN	0.70385	0.00004	0.00001	0.012	1274	0.703791 - 0.70403	1276 - 1547 µg/g 26 values (compiled: 1370 µg/g)
basalt	Geostandard ††	BEN bis	0.70380	0.00003	0.00001	0.010	1274	0.703791 - 0.70403	1276 - 1547 µg/g 26 values (compiled: 1370 µg/g)

lithology	SECTION	**Sample ID**	**$^{87}Sr/^{86}Sr$**	**sd**	**SE†**	**RSD§**	**Sr (µg/g)**	**$\delta^{13}C$ (‰)#**	**$\delta^{18}O$ (‰)#**
bulk $CaCO_3$	Monte Acuto	MMA-1	0.70754	0.00002	0.00001	0.005	212	1.87	-1.99
bulk $CaCO_3$	Monte Acuto	MMA-2	0.70758	0.00003	0.00002	0.008	214	1.73	-1.76
bulk $CaCO_3$	Monte Acuto	MMA-3	0.70755	0.00002	0.00001	0.006	202	1.81	-2.14
bulk $CaCO_3$	Monte Acuto	MMA-4	0.70750	0.00002	0.00002	0.006	213	2.01	-1.87
bulk $CaCO_3$	Monte Acuto	MMA-5	0.70753	0.00003	0.00002	0.008	213	2.02	-1.70
bulk $CaCO_3$	Monte Acuto	MMA-6	0.70748	0.00002	0.00002	0.007	224	2.05	-2.21
bulk $CaCO_3$	Monte Acuto	MMA-7	0.70751	0.00003	0.00002	0.008	251	2.36	-2.05
bulk $CaCO_3$	Monte Acuto	MMA-8	0.70749	0.00002	0.00002	0.006	208	2.65	-2.12
bulk $CaCO_3$	Monte Acuto	MMA-9	0.70746	0.00002	0.00001	0.006	233	3.15	-2.05
bulk $CaCO_3$	Monte Acuto	MMA-10	0.70748	0.00002	0.00002	0.006	260	2.92	-2.02
bulk $CaCO_3$	Monte Acuto	MMA-11.2	0.70751	0.00002	0.00001	0.005	252	2.88	-1.28
bulk $CaCO_3$	Monte Acuto	MMA-12	0.70741	0.00003	0.00002	0.009	257	2.39	-1.67
bulk $CaCO_3$	Monte Acuto	MMA-13	0.70741	0.00003	0.00003	0.010	264	1.56	-1.80
bulk $CaCO_3$	Monte Acuto	MMA-14	0.70742	0.00003	0.00002	0.009	255	1.38	-1.85
bulk $CaCO_3$	Monte Acuto	MMA-15	0.70739	0.00003	0.00002	0.007	228	1.32	-2.01

bulk $CaCO_3$	Monte Acuto	MMA-16	0.70738	0.00003	0.00002	0.008	208	1.42	-1.99
bulk $CaCO_3$	Monte Acuto	MMA-17	0.70737	0.00002	0.00002	0.007	240	1.34	-2.03
bulk $CaCO_3$	Monte Acuto	MMA-18	0.70734	0.00003	0.00002	0.008	280	1.58	-1.69
bulk $CaCO_3$	Monte Acuto	MMA-19	0.70738	0.00003	0.00002	0.009	232	1.37	-1.75
bulk $CaCO_3$	Monte Acuto	MMA-20	0.70733	0.00003	0.00002	0.009	228	1.56	-1.60
bulk $CaCO_3$	Monte Acuto	MMA-21	0.70737	0.00003	0.00002	0.007	217	1.52	-1.50
bulk $CaCO_3$	Monte Acuto	MMA-22	0.70737	0.00002	0.00002	0.006	208	1.56	-1.58
bulk $CaCO_3$	Monte Acuto	MMA-23	0.70733	0.00002	0.00002	0.006	228	1.42	-1.54
bulk $CaCO_3$	Monte Acuto	MMA-24	0.70736	0.00002	0.00002	0.007	197	1.45	-1.53
calcite vein	Monte Acuto	MMA-11.1	0.70762	0.00003	0.00003	0.010	448	2.10	0.46
replicate	Monte Acuto	MMA-1bis	0.70753	0.00003	0.00002	0.008	209	n.a.	n.a.
replicate	Monte Acuto	MMA-16bis	0.70741	0.00003	0.00002	0.008	n.a.	n.a.	n.a.
replicate	Monte Acuto	MMA-20bis	0.70733	0.00002	0.00002	0.007	226	n.a.	n.a.
replicate	Monte Acuto	MMA-1tris	0.70754	0.00004	0.00003	0.011	210	n.a.	n.a.
replicate	Monte Acuto	MMA-20tris	0.70735	0.00004	0.00003	0.010	231	n.a.	n.a.

lithology	Sample type	**Sample ID**	**$^{87}Sr/^{86}Sr$**		**SE**	**RSD**	**Sr (µg/g)**	**Reference value (GEoREM) $^{87}Sr/^{86}Sr$**	**Reference value (GEoREM) Sr (µg/g)**
basalt	Geostandard ⁺⁺	BE-N	0.70379	0.00005	0.00002	0.007	1407	0.703791 - 0.70403	1276 - 1547 µg/g 26 values (compiled: 1370 µg/g)
micro-gabbro	Geostandard ⁺⁺	PM-S	0.70467	0.00005	0.00002	0.007	265	0.704596	270 - 296 µg/g (compiled: 275 - 280 µg/g , 2 values)

*sd: standard deviation

†SE: standard error

§RSD: relative standard deviation

#all delta values are reported against V-PDB standard

** n.a. not analysed

⁺⁺geostandards obtained from Le Centre de Recherches Pétrographiques et Géochimiques (CRPG)

measured values for geo-analytical standards are in excellent agreement with reported values

J. BELZA FIGURE 1

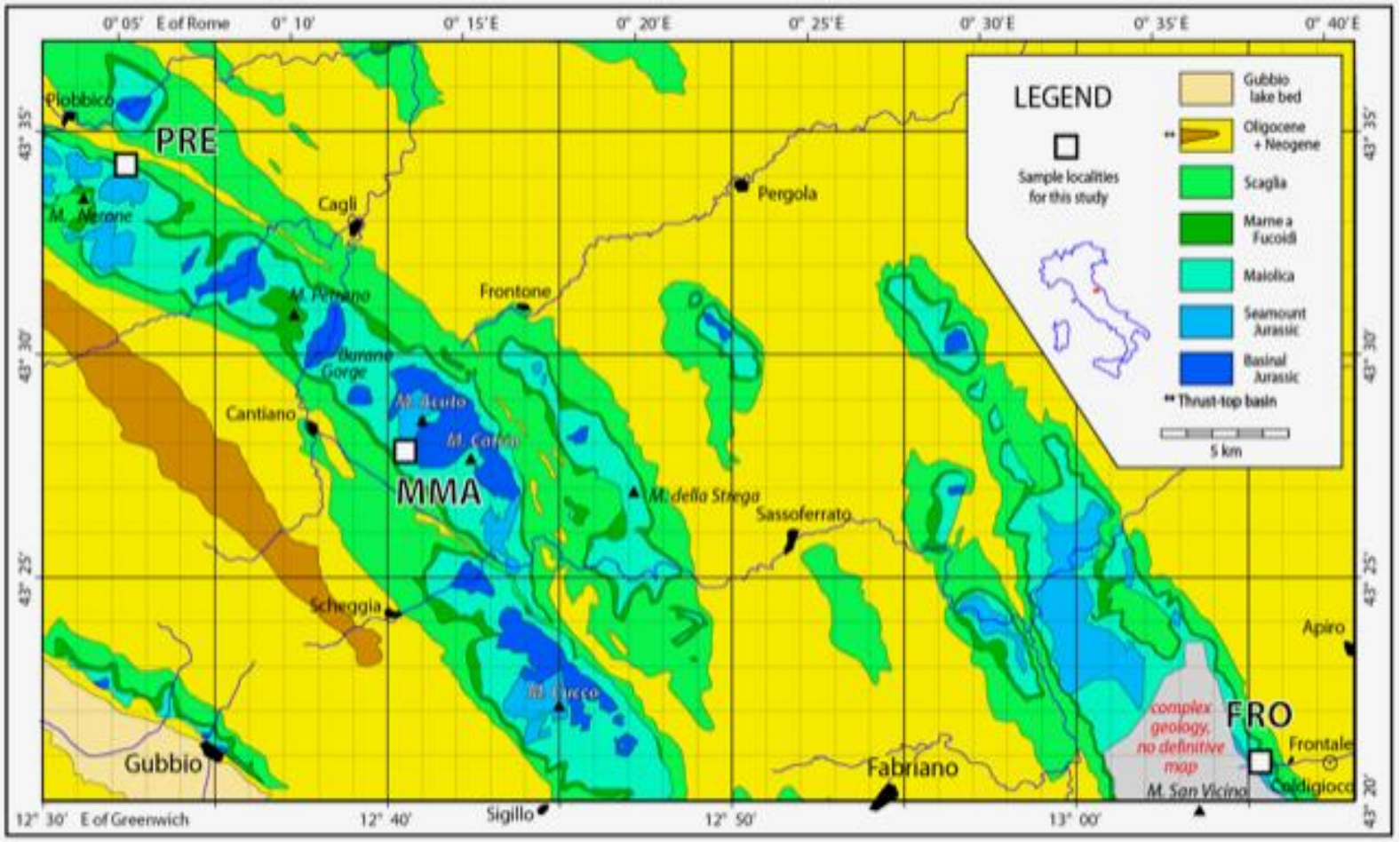

J. BELZA FIGURE 2

J. BELZA FIGURE 3

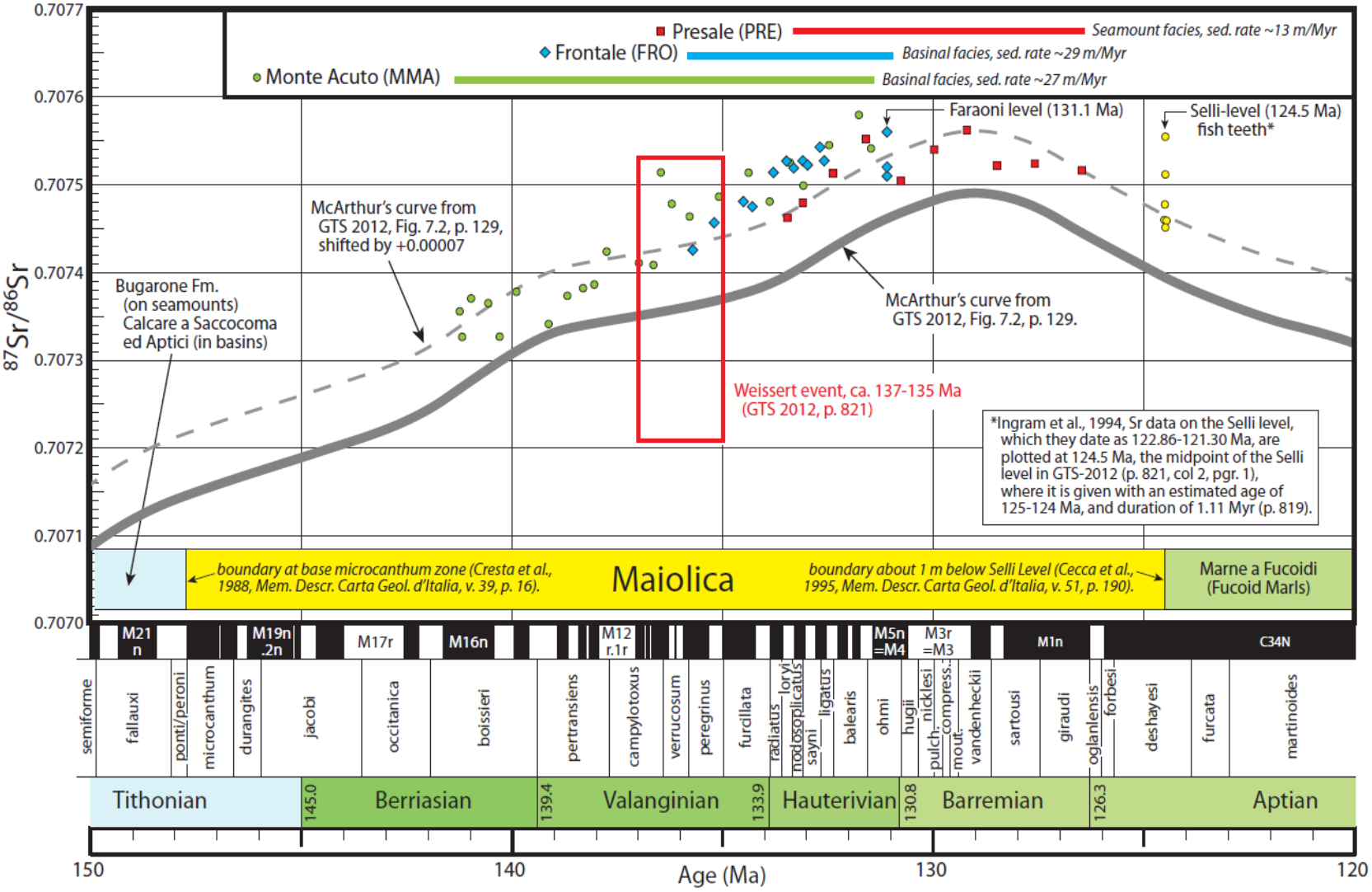

J. BELZA FIGURE 4

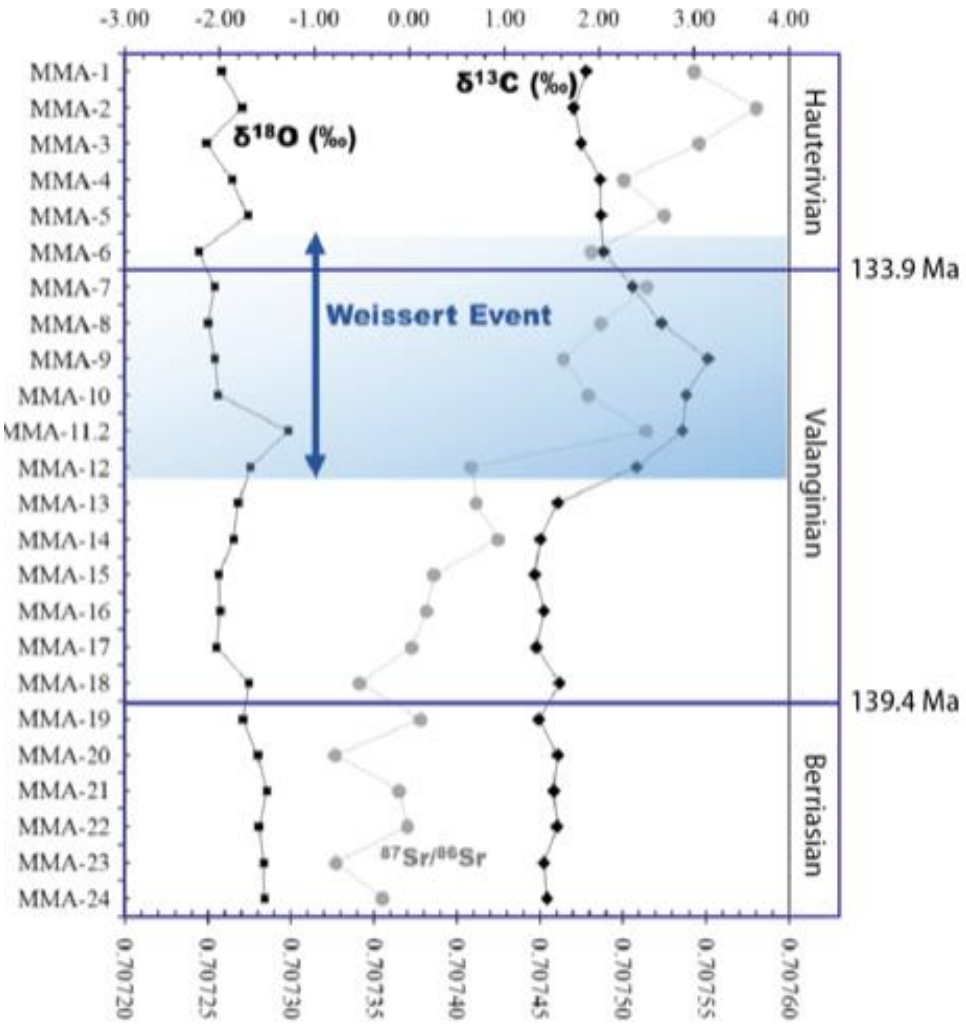

$^{87}Sr/^{86}Sr$ RECORD FROM THE LOWER CRETACEOUS PELAGIC MAIOLICA LIMESTONE (CENTRAL APENNINES, ITALY) AND ITS OFFSET FROM THE GLOBAL SEAWATER REFERENCE CURVE~~:~~ ~~INTERPRETATION CONSTRAINED BY WHOLE ROCK CARBONATE DATA~~

J. Belza[1*], W. Alvarez[2], F. Vanhaecke[1], P. Claeys[3]

[1]Department of Chemistry, Atomic and Mass Spectrometry (A&MS) research unit, Ghent University, Campus Sterre, Krijgslaan 281 – S12, 9000 Ghent, Belgium,

[2]Dept. Earth and Planetary Science, University of California Berkeley, CA 94720-4767 USA, and Geological Observatory of Coldigioco, Contrada Coldigioco, 62020 Frontale di Apiro, Italy.

[3]Dept. Analytical Environmental and Geo-Chemistry (AMGC), Vrije Universiteit Brussel, Pleinlaan 2 1050 Brussels, Belgium~~,~~

*Corresponding author: jbelza@vub.ac.be

Field Code Changed

Formatted: Font color: Auto

ABSTRACT

This study provides a composite record of $^{87}Sr/^{86}Sr$, $\delta^{18}O$ and $\delta^{13}C$ for three sections in the Tethyan Lower Cretaceous Maiolica formation, a pelagic limestone from the Umbria-Marche Apennines of Italy, carefully tied to a magnetostratigraphically and biostratigraphically calibrated timescale. Although the $^{87}Sr/^{86}Sr$ record accurately follows the trend of the global marine $^{87}Sr/^{86}Sr$ reference curve ~~McArthur Sr seawater reference curve~~, individual Sr isotope

ratio values are relatively high for their inferred stratigraphic position, with all $^{87}Sr/^{86}Sr$ ~~isotope ratios~~ ratios ~~–~~yielding a fairly uniform +0.00007 to +0.0001 discrepancy. This offset likely results from incorporation of excess ^{87}Sr through isotopic re-equilibration with interstitial pore waters during progressive lithification of the calcareous ooze. Although the process occurs principally through dissolution-reprecipitation, buffering the contemporaneous seawater Sr isotopic signature, diffusive communication with the overlying water column and porous sediments will compete with the dissolution-precipitation process, homogenizing pore fluid concentrations and isotope ratios throughout the sediment column. Because the secular trend in $^{87}Sr/^{86}Sr$ throughout the Maiolica timeframe is one of constant increase before rebounding to lower $^{87}Sr/^{86}Sr$ ratios in the Barremian, the ratios of the Maiolica carbonates are systematically displaced from that of the seawater in which it was deposited towards more radiogenic (higher $^{87}Sr/^{86}Sr$) values. In addition, the carbon and oxygen isotope ~~ratio seawater~~ record of the Maiolica allows identification of the Mid-Valanginian Weissert event, characterized by a positive excursion in the $\delta^{13}C$ and the $\delta^{18}O$ record. Furthermore, the Weissert event correlates with a positive spike (+0.0001) in $^{87}Sr/^{86}Sr$, ~~.~~Both the Sr and O isotopic peak signal pre-date the maximum peak in the $\delta^{13}C$ excursion. This is likely a diagenetic artefact and ~~further strengthens~~ may support the hypothesis of diffusive communication during lithification of the calcareous ooze. ~~Nonetheless, our O, C and Sr isotope ratio data support earlier hypotheses on the origin of the Weissert event, characterized by the increase in atmospheric CO_2 resulting from the eruption of the Paraná-Etendeka traps, triggering accelerated weathering and providing an indirect nutrient flux to and fertilization of the oceans.~~

Formatted: Superscript

Formatted: Superscript

1. INTRODUCTION

1.1 The Umbria-Marche sequence

The stratigraphic sequence of the Umbria-Marche Apennines in central Italy offers a world-class archive of information about Earth history from the Pliensbachian, in the early Jurassic, ~~Early Jurassic,~~ to the Miocene in the Neogene ~~to the Miocene~~ (Cresta et al., 1989; Montanari and Koeberl, 2000; Alvarez, this volume). This is due to the pelagic character of these limestones, marls, and cherts, which were deposited on the thinned, subsided Italian continental crust at moderate oceanic depth, just above or just below the calcite compensation depth. Because of these conditions, the Umbria-Marche sequence lacks terrigeneous inputs until the Oligocene, is free of wave erosion, and was rarely affected by current scour. Equivalent pelagic oozes have been cored by scientific drilling ships at many sites throughout the world ocean, where they have the advantage of not having been compacted, uplifted, or placed in contact with non-marine pore waters. In compensation, the Umbria-Marche carbonate rocks are extensively exposed across whole mountain sides in a region of broad anticlinal folds covering about 5,000 km^2, so that lateral relationships can be studied and two-dimensional sampling can be carried out, neither of which is possible with deep-sea cores. Because pelagic carbonate rocks have usually either stayed at depth below the sea or been strongly deformed during tectonism and uplift, the Umbria-Marche Apennines are ~~unique~~ ideal for the study of pelagic carbonates in outcrop~~; no other large, well-preserved area of this kind of rocks is known~~.

The great majority of stratigraphic research in the Umbria-Marche Apennines has focused on the ca. 600 m thick Scaglia formations — the Scaglia bianca, rossa, variegata, and cinerea —

Formatted: Font color: Auto

beginning with white pelagic limestone in the Cenomanian, then pink pelagic limestone from the Turonian to the Eocene, and transitioning to a grey pelagic marl in the Oligocene. The Scaglia has been of great stratigraphic use because of the abundance of recognizable lithologic contacts and marker beds and of planktic foraminifera, and has led to advances in magnetic polarity stratigraphy, radioisotopic dating of intercalated volcanic ash beds, isotopic stratigraphy, event stratigraphy, including recognition of the Cretaceous-~~Paleo~~Palaeogene boundary impact event, and cyclostratigraphy (Coccioni and Montanari, this volume).

Turning to the Lower Cretaceous, less attention has been paid to the Aptian-Albian Fucoid marls (Grippo et al., 2004). The Tithonian-to-Albian Maiolica limestone (Sprovieri et al., 2006) has been particularly intractable, because of the 1) 400 m thickness of uniform lithology of white limestone with beds and nodules of black chert, 2) ~~because of~~ the presence of only a single recognizable ~~marked~~ marker bed, and ~~because of~~3)- the absence of the ~~not yet evolved~~ planktic foraminifera, which had not yet evolved. Although the Maiolica ~~gives~~ yields good ~~paleo~~palaeomagnetic directions, magnetic-polarity stratigraphy has been difficult to apply to the Maiolica~~?~~ because the M-sequence reversals, covering almost all of the Maiolica, contain many short polarity zones with no distinctive long zones, making it hard to correlate a particular set of polarity zones in the Maiolica to the M-sequence reversals (Lowrie et al., 1980).

The overall architecture of the Maiolica shows a division into basinal sequences, typically ~400 m thick, and thinner sequences, ~100 m thick, on the tops and margins of fault-block seamounts (Alvarez, 1989). The seamount sequences are incomplete because of stratigraphic hiatuses, and in compensation, the basinal sequences commonly contain frequent levels of slumps. In the present paper we report on the study of one seamount and two basinal sequences.

The present study began with an attempt to use $^{87}Sr/^{86}Sr$ ratios as a correlation tool for the Maiolica. Specifically it aimed at providing a detailed stratigraphic framework to investigate near-vertical walls of shattered breccia in the Maiolica formation, for which a hydraulic fracturing mechanism seems likely. In two companion papers (Alvarez et al., this volume; Belza et al., this volume), we detail the structural observations and geochemistry of these breccia walls, which are exposed along the anticlines of the Umbria-Marche Apennines thrust-and-fold belt. The breccias are mostly confined to the Maiolica formation, and are characterized by bodies of shattered pelagic limestone. Our goal was to determine, using $^{87}Sr/^{86}Sr$ ratios, whether the Maiolica breccia fragments have moved up or down, and how far, relative to the stratigraphic level where they now reside. The standard global marine $^{87}Sr/^{86}Sr$ reference curve (McArthur et al., 2012, Fig. 7.2) shows a monotonic rise from ~0.70715 to ~0.70750 in the first 80% of the Maiolica, followed by a decrease to ~0.70740 at the top of the formation. The long monotonic increase gave reason for hope that the strontium isotope ratio values in breccia fragments could identify their original stratigraphic position.

First, however, it would be necessary to test whether the Maiolica accurately records the global strontium-isotope reference curve for the Lower Cretaceous. The present study was undertaken to do this testing, and it unexpectedly showed that the $^{87}Sr/^{86}Sr$ values in the Maiolica, although they show the same pattern of a long rise followed by a shorter fall, are systematically offset by about +0.0001 relative to the global curve. Thus, our attempt to study the origin of the Maiolica breccias has been diverted into an attempt to understand the offset in the Maiolica strontium isotope ratio curve.

Our attempt to tie the $^{87}Sr/^{86}Sr$ record to the global Sr seawater reference curve was only possible because of the unique stratigraphic control of the sections studied: the pelagic

limestones in the Umbria-Marche Apennines have been extremely well dated because of 1) the presence of microfossils and nanofossils 2) magnetic minerals recording the geomagnetic polarity3) and the presence of levels of distal volcanic ejecta that can be dated radiometrically, which made it possible to tie all three major geological dating methods in one sedimentary succession (Alvarez, 2009). As such the stratigraphic positions of our samples were accurately determined by tying them to the magnetic polarity stratigraphy (Channel et al., 1995; Lowrie and Alvarez, 1984) and biostratigraphy (Cecca et al., 1994, Fig. 2, column 22; Faraoni et al., 1997 Coccioni et al., 1998). This was accomplished by identifying the old paleomagnetic drill holes in the succession and using the core orientations provided James E. Channel (personal communication).

1.2 Chemostratigraphy

~~In all, c~~Changes in ocean chemistry are controlled by fluctuating global weathering rates, by changes in volcanic and hydrothermal activity and by sedimentological and tectonic processes (Weissert et al., 2008). The variation in the past ~~isotopic~~ composition of seawater over geological time is recorded in the $\delta^{13}C$, $\delta^{18}O$, $^{87}Sr/^{86}Sr$ ratios of marine carbonates, and serves as a reliable stratigraphic tool for global correlation. In addition, the Sr, O and C isotopic signatures are useful in constraining post-depositional diagenetic events, an important factor that may obscure the targeted stratigraphic resolution. This is especially relevant for the oxygen isotopic system, as the $\delta^{18}O$ of the carbonate depositing from the fluid is temperature-dependant.

Formatted: Font color: Auto

1.2.1 Carbon Isotope Ratio Stratigraphy

Because ~~precipitation of carbonates occurs without significant carbon isotope fractionation relative to dissolved inorganic carbon (DIC), and~~ the $\delta^{13}C$ of carbonate is relatively insensitive to changes in temperature, the $\delta^{13}C$ isotopic signature of inorganically and biologically precipitated carbonate will reflect the (fractionated) $\delta^{13}C$ of dissolved inorganic carbon (DIC) of seawater at the point of calcification and can be used to trace changes in ocean circulation and ~~paleo~~palaeoproductivity (Zeebe and Wolf-Gladrow, 2001; Edgar et al., 2013). The $\delta^{13}C$ value of whole-ocean DIC has not been constant over geologic time. Variations in $\delta^{13}C$ in the DIC in the oceans over time reflect redistribution of carbon among the Earth's surface carbon reservoirs such as the atmosphere, oceans, biosphere and lithosphere (Sundquist and Visser, 2003). This includes factors driven by changes in atmospheric CO_2 or DIC levels in the ocean, such as changes in bioproductivity and~~,~~ organic carbon burial~~, all factors driven by changes in atmospheric CO_2 or DIC levels in the ocean.~~

1.2.2 Oxygen Isotope Ratio Stratigraphy

Oxygen isotope ratios in marine carbonate vary as a function of both the temperature and the $\delta^{18}O$ composition of the parent seawater (; Shackleton, 1967). The strongly temperature-dependent calcite-water oxygen isotope fractionation has been well-established by numerous empirical, experimental and theoretical studies. Increasing temperatures shift $\delta^{18}O$ values in marine calcite to more negative values. Combined with ~~paleo~~palaeontological information, $\delta^{18}O$ values serve as a reliable proxy for changes in ~~paleo~~palaeo-ocean temperatures, salinity, and global ice volumes (Shackleton, 1967; Veizer et al., 1986; Rohling and Bigg, 1998; Veizer et al., 1999; Edgar et al., 2013). As ocean temperatures vary with depth and latitude, oxygen isotope records will depend on ~~paleo~~palaeogeography and depth habitat of the calcifying microorganisms (Grossman, 2012).

Formatted: Font color: Auto

Because the oxygen and carbon isotope signals in this study were measured on bulk carbonates, they might be sensitive to changes in the community of carbonate producers and diagenesis. This will be highlighted in the Discussion section.

Formatted: English (United States)

1.2.3 Strontium Isotope Ratio Stratigraphy

The $^{87}Sr/^{86}Sr$ value~~isotope ratio~~ of seawater has been recognized to be a diagnostic tool for stratigraphic correlations, reconstruction of global tectonics, ~~paleo~~palaeo-climatic perturbations, and understanding of diagenetic processes (Burke et al., 1982; Veizer, 1989; McArthur et al., 2001; McArthur et al., 2012). The principle of strontium isotope ratio stratigraphy relies on the fact that the Sr isotopic composition of the oceans has varied throughout geological time, due to variation of two main sources contributing Sr to the oceans: (1) hydrothermal exchange of seawater with volcanic rocks on the ocean floor (Frijia and Parente, 2008), and (2) diagenesis and continental weathering of old marine limestones and weathering of old granitic rocks delivering strontium to the oceans by river influx (Faure and Powell, 1972~~)).~~

Because the residence time of Sr in the oceans (10^6 years) is much longer than the time it takes currents to mix the oceans (10^3 years), oceans are thoroughly mixed on time scales that are short relative to the rates of gain and loss of strontium. As a result, the isotopic composition of strontium is considered to be constant throughout the global ocean at any one time (Veizer 1989; Palmer and Edmond, 1989). Because Sr^{2+} substitutes for Ca^{2+} during precipitation of marine carbonates and sulphates with minor~~out~~ isotope fractionation, the $^{87}Sr/^{86}Sr$ ratio of marine carbonates will reflect the isotopic ratio of the contemporary seawater during precipitation (Faure and Powell, 1972,.). Based on this assumption, Howarth and McArthur (1997) and McArthur et al. (2001) have compiled $^{87}Sr/^{86}Sr$ data and fitted to them a

nonparametric LOWESS statistical regression function (Locally, Weighted Scatterplot Smoother), resulting in a global strontium seawater reference curve (McArthur et al., 2012).

With carbon isotope ratio data providing information on the evolution and perturbation of the global carbon cycle, and $\delta^{18}O$ isotope data, combined with palaeontological information, potentially serving as a palaeotemperature proxy (Weissert and Erba, 2004), the combination with strontium isotopic data provides a powerful chemostratigraphic tool to constrain the link between (continental) weathering, volcanism, tectonics and ~~paleo~~palaeoclimatic perturbations, and document the temporal response of different isotopic systems on the Tethys carbonate sedimentation to the environmental perturbations.

1.3 Sections sampled

Most of the detailed sampling of Umbria-Marche pelagic limestone formations over the years has been done along roads because of the long, continuous sections, the fresh outcrops, and the exposure of easily erodible marl and shale layers (Lowrie et la., 1980; Alvarez et al.; 1977a, 1977b; Cecca, 1994; Cecca, 1995; Alvarez, 2009; Coccioni and Montanari, 2018)~~.~~ There are many such road-cut section~~s~~s of the Scaglia, notably the Bottaccione and Contessa sections at Gubbio (several papers in this volume). The Maiolica offers fewer such usable sections; we have studied three of those available. The Monte Acuto (MMA) and Frontale (FRO) sections expose parts of the thick, basinal facies Maiolica, while the Presale (PRE) section exposes the thin, seamount facies. Sample localities are ~~depicted~~ shown in Fig. 1.

1.3.1 Monte Acuto section (MMA)

Formatted: Font color: Auto

The Monte Acuto section (MMA in this paper), located along the road from Chiaserna up to the pass between Monte Acuto and Monte Catria, exposes the lower 240 m of the Maiolica, with the upper part covered (Fig. 2). The complete stratigraphic record of the section extends from the middle Berriasian to the upper Hauterivian. Three thin black shale layers occur interbedded within the limestone beds (Sprovieri et al., 2006). The Maiolica sequence at the Monte Acuto section is cut by calcite-filled veins.

This excellent section represents the thick, basinal Maiolica, and it has been important for previous stratigraphic research on the Maiolica. The magnetic polarity stratigraphy together with ammonite and nannofossil biostratigraphy were studied by Channell et al. (1995), the rare ammonites by Cecca (1995) and Faraoni et al. (1997), and the cyclostratigraphy by Sprovieri et al. (2006).

In October 2012, we collected 24 samples, from MMA-1 (at the lowest road elevation, but highest in the stratigraphy, at 43°27'49.80"N, 12°40'16.17"E), to MMA-24 (at the highest road elevation, but lowest in the stratigraphy, at 43°27'50.52"N, 12°40'44.70"E; coordinates from Google Earth, not from GPS). Our sample sites are marked with small numbers in green paint. The positions of our samples MMA-1 to MMA-10 have been tied to the magnetic polarity stratigraphy of Channell et al. (1995) and thus dated, based on identifying the ~~paleo~~palaeomagnetic drill holes, using the core orientations supplied by James E. Channell (personal communication, 2013). Stratigraphically, below MMA-10 there is a 20-30-m-wide covered interval which marks the bottom of the ~~paleo~~palaeomagnetic section of Channell et al. (1995).

In subsequent work by Faraoni et al. (1997) and Sprovieri et al. (2006), a prominent chert marker bed was recognized on both sides of the covered interval and painted blue, making it possible to continue the section downward below the base of the ~~paleo~~palaeomagnetic section, and this lower part of the section was tied to the global biostratigraphy using very rare ammonites Faraoni et al. (1997). Our samples MMA-11 to MMA-24 were taken in this lower part of the section, and were dated using the biostratigraphy of Faraoni et al. (1997).

1.3.2 Frontale section

A second section was sampled on the road from Frontale to Pian dell'Elmo. This basinal Maiolica was well exposed when the road cuts were fresh and was used for a ~~paleo~~palaeomagnetic stratigraphy study by Lowrie and Alvarez (1984). Sometime in the 30 years since that study, the road cuts were covered by heavy screening. During the screening work, many core holes were cut away, and subsequently many others were covered by debris trapped behind the screen. However, we were able to identify enough of the remaining cores holes by their orientations (data from William Lowrie, personal communication, 2013) to re-measure the original section, confirming the location of two faults noted by Lowrie and Alvarez (1984). The meter levels of the recovered section have now been marked with green paint on the outcrop behind the screen, and on the metal guard-rail on the opposite side of the road.

We took 23 samples for isotopic analysis, numbered with their meter levels, from FRO-470 (at the highest road elevation, but lowest in the stratigraphy, at 43° 20.949'N, 13° 5.055'E), to FRO-597 (at the lowest road elevation, but highest in the stratigraphy, at 43° 20.885'N, 13° 5.348'E; coordinates from Google Earth, not from GPS). Because of the presence of two prominent faults in the section (Lowrie, 1984— the "Big Fault" and the "Culvert Fault," the latter with its lowest exposure at a road culvert — not all of the samples were useful for the present

stratigraphic study. The useful samples are FRO-470 through FRO-561, located in the long, unfaulted lower part of the section, which is dated by the magnetic polarity zones of Lowrie and Alvarez (1984), and FRO-565, 566, and 568, located in the block between the two faults, datable because it contains the upper Hauterivian Faraoni level (Cecca et al., 1994, Fig. 2, column 22; Coccioni et al., 1998).

1.3.3 Presale section

Since neither the Monte Acuto nor the Frontale section extends to the top of the Maiolica, we also sampled the Presale section, which seems to have been studied previously only by Lowrie and Alvarez (1984). This section is exposed along a trail 3.15 km southeast of the bridge at the main road junction in Piobbico. We were able to relocate several of the original painted numbers corresponding to every 5 m in the 1984 magnetic stratigraphy section, although these green numbers are very faded and hard to see. Also recognizable are some of the supplementary green-painted meter marks (a line and 1, 2, 3, or 4 dots, corresponding to that many meters above a painted number).

We collected 10 samples, from the stratigraphically lowest, PRE-1 (43° 34.159'N, 12° 32.295'E, 170 m in the 1984 section), to PRE-10 (43° 34.195'N, 12° 32.346'E, 260 m in the 1984 section; coordinates from Google Earth, not from GPS). These samples are well dated because they are tied to the polarity stratigraphy of Lowrie and Alvarez (1984). It should be noted that the Presale Maiolica section is only about 100 m thick, which is typical of the thin Maiolica on the Jurassic fault-block seamounts, rather than the ~450 m found in basinal sections like Monte Acuto and Frontale (Alvarez, 1989; Cresta, 1989, p. 23-25).

2. METHODS

Bulk carbonate sample powders were extracted using a dental drill with a tungsten-carbide drill bit. In between drilling of different samples, the drill and drill bit were carefully cleaned with pressured air, ethanol and ultrapure 18.2 MΩ.cm water to avoid cross-contamination. Drilling was carried out using a drill bit of 0.5 mm in order to prevent sparry calcite cement ~~and~~ from visible calcite veins~~- ,-~~yielding a different isotopic signature, to mix with the limestone powders. Furthermore, sparry, calcite-cemented veins were separately sampled as well.

2.1 ~~Strontium isotope ratio~~87Sr/86Sr

For Sr isotopic analysis of the carbonates, 100 mg of sample powder was accurately weighed in pre-cleaned Teflon® beakers. Next, 5 mL of 1M HCl was added to dissolve the samples. Along with the samples, one NIST SRM 987 $SrCO_3$ standard (National Institute for Standards and Technology, USA), several procedure blanks and sample duplicates were dissolved as well. Sample solutions appeared clear after dissolution with almost no visible residue. However, to fully eliminate any possible contribution from radiogenic ^{87}Sr leached from clay fractions in following steps involving concentrated strong acid attack, the solutions were centrifuged. After centrifugation, clear supernatant solutions were pipetted off and transferred to clean Teflon® vials. Next, the solutions were evaporated to near-dryness on a hotplate at 70°C and redissolved in 2mL of 7 M HNO_3. In addition, two samples (MMA-1tris and MMA-20tris) were subjected

Formatted: Font color: Auto

to a different dissolution procedure by adding 2 mL of 7 M HNO_3 instead of 5 mL of 1 M HCl. This was done in order to evaluate the influence of the use of highly concentrated acids (such as concentrated nitric acid) throughout the extraction procedure on the possible leaching of radiogenic Sr from the remaining clay fraction in the carbonate powders. Also, two international (silicate) rock reference standards (the basalt BE-N and micro gabbro PM-S obtained from the Centre de Recherches Petrographiques et Géochimiques) were prepared following a different digestion protocol: 100 mg of sample powder was accurately weighed in clean Teflon® beakers and digested by addition and subsequent evaporation of 1) HF:HNO_3 (in a ratio of 2:4, 14 M HNO3 and 28M HF), (2) *Aqua regia*, (3) 14 M HNO_3 (4) 14 M HNO_3. Finally, the sample was redissolved in 7 M HNO_3.

The Sr was extracted using pre-packed BioRad columns, filled with 400 µL of the commercially available strontium-specific extraction chromatographic resin Sr spec™, and following an optimized procedure of De Muynck et al. (2009). $^{87}Sr/^{86}Sr$ ratios were subsequently measured using a Neptune multi-collector ICP-mass spectrometry (MC-ICP-MS) instrument at the Department of Chemistry at Ghent University. All samples were run in a sample-standard bracketing sequence with a 100 µg/L Sr isotopic standard solution of NIST SRM 987 $SrCO_3$. The Sr content in the samples and the standard was matched within ±10% to avoid any effect from the analyte content on the extent of instrumental mass discrimination. After every run, the sample introduction system was rinsed thoroughly with 2% HNO_3 to minimize memory effects. The results were mathematically corrected for mass bias using internal normalization to $^{86}Sr/^{88}Sr=0.1194$ by the exponential fractionation law.. The intensities obtained for $^{82}Kr^+$, $^{83}Kr^+$, and $^{85}Rb^+$ were used to correct for the Kr interferences on the m/z ratios of 84 and 86, and for the Rb interference on the m/z ratio of 87. The mean, long-term $^{87}Sr/^{86}Sr$ ratio obtained for NIST SRM 987 $SrCO_3$ was 0.710287 ± 0.000024 (2s.e., with N = 44). This is in full agreement

with the accepted $^{87}Sr/^{86}Sr$ ratio of 0.710248 ±0.000011 (2s.d.) for this reference material (Thirlwall, 1991).

2.2 Carbon and oxygen isotope ratios

Carbon and oxygen isotope ratios were measured both with a Kiel-III-device coupled to a Thermo Delta plus XL isotope ratio mass spectrometer, and a a NuCarb automated carbonate preparation device ~~-~~coupled to a Nu Perspective Isotope Ratio Mass Spectrometer~~-coupled to~~. Small quantities of carbonate powder were reacted with ~~orthophosphoric acid~~H_3PO_4 at a temperature of 75°C and the CO_2 generated was cryotrapped. Every set of six samples was bracketed by an international calcite standard (NBS-19 with $\delta^{18}O$ = -2.20 ± 0.01, $\delta^{13}C$ =+1.95 ± 0.02, or the NCM with $\delta^{18}O$ = -1.9 and $\delta^{13}C$= +2.09). Moreover, every sample was analysed three or four times on different measurement days. Carbon and oxygen isotopic results are reported on a per mil (‰) basis relative to the Vienna Pee Dee Belemnite (VPDB) standard. External analytical precision yielded values better than ± 0.015 ‰ for $\delta^{13}C$ and ±0.033‰ for $\delta^{18}O$ based on replicate analysis of the international calcite standards NBS-19 (US Geologicl Survey-USGS) and the in-house NCM (Cararra Marble, Nu instruments). Precision is reported as 1-sigma standard deviation.

Formatted: Superscript

Formatted: Font color: Auto

Formatted: Subscript

Formatted: Subscript

3. RESULTS

3.1 Strontium, oxygen and carbon isotopic results

3.3.1 $^{87}Sr/^{86}Sr$

$^{87}Sr/^{86}Sr$ ~~isotope~~ ratios vary between 0.70733 and 0.70758 (Tables 1, 2). The Sr isotopic trend accurately follows the McArthur seawater reference curve for the inferred stratigraphic interval (Late Berriasian ~141 Ma to Late Barremian ~127 Ma), but individual Sr isotope ratios are offset by +0.00007 to +0.0001 (Fig. 3). ~~,~~The $^{87}Sr/^{86}Sr$ of the calcite veins is much higher than the values of their host rock, yielding values between 0.70762-0.70777.

3.3.2 $\delta^{13}C$

Carbon isotope ratios cluster around plateau values of ~1.5‰ in the Berriasian to Early Valangian (Table 1, Fig.4). In The Mid-Valangian, $\delta^{13}C$ values rise rapidly to ~3‰~~.~~ This positive C-isotopic of 1-1.5‰ excursion starts in the Valanginian *campylotoxus* ammonite zone, reaches peak values in the *verrucosum* zone and ends in the Hauterivian *radiatus* zone, corresponding to polarity chrons CM12–CM9 (Channell et al. 1993; Hennig et al. 1999; Weissert and Erba, 2004). Furthermore, this carbon isotopic excursion correlates with the well-defined Weissert Event, which is characterized by a positive $\delta^{13}C$ excursion of about 1 to 2‰ in marine carbonates. (Weissert and Erba, 2004), the first of four positive excursions recorded in the Cretaceous carbon isotopic record. In the Hauterivian, the $\delta^{13}C$ isotopic signature falls back to a background value of approximately ~2‰. Furthermore, carbon isotopic values in calcite veins reflect values of their host rock, ~~and have remained unchanged~~suggesting they were buffered by the host rock during deposition of secondary calcite.

3.3.3 $\delta^{18}O$

Oxygen isotope ratio values range between -2.25‰ and -1.5‰ (Table 1). Compared to ~~paleo~~palaeogeographically comparable, selected sections from the Southern Alps (Weissert et al., 1985; Weissert and Channell, 1989), the oxygen values are depleted by approximately -1‰. On the other hand, oxygen isotope ratio values of the calcite veins document significant enrichment in the heavy ^{18}O and mostly yield positive $\delta^{18}O$ values, ranging between -0.65 to 2.44 ‰.

3.3.4 $^{87}Sr/^{86}Sr$, $\delta^{18}O$, $\delta^{13}C$ composite record

A composite strontium, carbon and oxygen isotope ratio record from Middle Berriasian to Late Barremian is presented in Fig. 4. Although broad and not very sharply bounded in our section, we can pinpoint the Mid-Valanginian positive excursion in the carbon isotopic record, identified as the Weissert Event, which correlates with a small (+0.0001), but resolvable positive spike in the $^{87}Sr/^{86}Sr$ curve. This excursion is very brief (~1 Ma) . In addition, the oxygen isotopic data yield a positive excursion with peak values corresponding exactly with the Sr spike. In the composite diagram, it can be seen that peak value of the carbon excursion, which covers approximately 5 Ma, is delayed with respect to the oxygen and Sr isotopic signal, which, in addition, cover a much smaller interval of time.

4. DISCUSSSION

4.1 Reliability of the $^{87}Sr/^{86}Sr$, $\delta^{13}C$ and $\delta^{18}O$ values

Before interpreting the isotopic records, it is important to assess whether the primary seawater isotopic values have been altered during post-depositional diagenetic processes and/or sample pre-treatment.

4.1.1 Oxygen isotope ratios

The process of recrystallization-dissolution will cause the $\delta^{18}O$ and the $\delta^{13}C$ of the carbonate to reequilibrate with the dissolved bicarbonate and the oxygen of the pore water. The Oxygen isotope ratios are most easily affected by diagenetic alteration. This is not solely because of a strong temperature-dependent fractionation, driving the $\delta^{18}O$ toward lower values as *in situ* temperature increases with sample depth in the sediment column (Matter et al., 1975; Schrag et al., 1995; Edgar et al., 2013). ~~In addition, in highly porous sediments, the pore water contains much more oxygen than the carbonate host and will largely influence the $\delta^{18}O$ ratio of the recrystallized calcite.~~ The lack of a "buffering" potential for oxygen during fluid-rock interaction is also due to huge amount of oxygen in water compared to the amount of dissolved carbonate in solution, and the relatively fast isotopic re-equilibration of oxygen in bicarbonate with oxygen in water.

4.1.2 Carbon isotope ratios

Compared to $\delta^{18}O$, the carbon isotope ratio values in carbonate rocks are less affected by diagenetic alteration. There is no (significant) temperature-dependent fractionation, and the $\delta^{13}C$ value is only measurably affected when recrystallization and cementation occur in the presence of pore water bicarbonate in which the $\delta^{13}C$ has been altered due to the addition of ^{12}C-enriched CO_2 derived from the oxidation of organic matter and microbial activity

(Marshall, 1992; Maliva et al., 1995; Maliva and Dickson, 1997; Madhavaraju et al., 2013). Also, because the carbonate contains considerably more carbon than the pore waters, the $\delta^{13}C$ value of the recrystallized carbonates will be buffered by the host limestone and remain relatively unaltered. Indeed, excellent agreement between our data and the established $\delta^{13}C$ reference curves (Fig.4; Weissert and Erba, 2004; Sprovieri et al., 2006) from the ~~Paleo~~Palaeo-Tethys indicates that the $\delta^{13}C$ value of the carbonate ~~is pristine and~~ was not altered by the contribution of carbon from a secondary source. ~~In addition, cross-plots (Fig. 5) of bulk carbon and oxygen isotopic values indicate a low covariance between $\delta^{13}C$ and $\delta^{18}O$ (R^2= 0.0256), hinting at minimal diagenetic modification.~~

Formatted: Font color: Auto

4.1.3 Strontium Isotope ratios

Several processes may account for the elevated $^{87}Sr/^{86}Sr$ with respect to the seawater reference curve. In the following paragraph, these processes are discussed in light of diagenetic modifications, analytical bias and sample contamination.

As a first possible explanation, if the modified $^{87}Sr/^{86}Sr$ ratios were derived from pressure solution deeper in the stratigraphic column or expulsion of fluids derived from structurally lower formations, we would expect a shift to more negative $^{87}Sr/^{86}Sr$ ratios, based on the Sr seawater reference curve (McArthur et al., 2001), (Fig. 1). On the other hand, deep-burial diagenesis or hydrothermal fluid circulation of deep brines would shift the $^{87}Sr/^{86}Sr$ towards higher values, as deep brines usually acquire an excess of ^{87}Sr from interactions with clays or other silicate minerals, imparting this signature into late cements (Veizer, 1989). However, deep burial diagenesis would significantly shift the $\delta^{18}O$ value to more negative values, which is not consistent with our observations.

A second possible source of ^{87}Sr that could have offset the $^{87}Sr/^{86}Sr$ by +0.0001 is the presence of abundant, parallel calcite veins, which yield $^{87}Sr/^{86}Sr$ +0.0001-0.0002 higher compared the host Maiolica carbonate. However, the calcite-cemented veins yield positive $\delta^{18}O$ values. If sub-mm calcite cemented veins had been accidentally sampled during micro-drilling and contaminated the carbonate powders, this would cause a measurable shift towards higher (more positive) $\delta^{18}O$ ratios of the bulk as well. This is not consistent with our data, which indicate that oxygen isotope ratios, if altered by diagenetic processes, would have shifted to slightly more positive values. Also, although one~~the~~ calcite vein~~s~~ contains an elevated Sr content compared to the host rock (Table1; PRE-3C), ~~concentrations are only 1.5-2-fold higher than those~~in other samples (FRO485C, FRO562.5C, MMA11.1, Table 1) concentrations are not much higher than the ~~in the~~ bulk rock from which the veins were sampled. In significantly higher concentration of Sr is required to affect the 87Sr/86Sr values of the bulk. In addition, the $^{87}Sr/^{86}Sr$ signature in other samples whit co-exisiting analysed veins (set for sample FROM485, FRO562.5, PRE-3) do not show spikes in the reconstructed $^{87}Sr/^{86}Sr$ record for the Maiolica., ~~C~~contamination from calcite veins requires this secondary calcite to represent a volumetrically significant component, which is not consistent with our observations.

A third possible candidate source for the observed increase in radiogenic Sr in the set of samples investigated may arise during the sample preparation and digestion procedure. Whole-rock carbonates may contain a negligible to large non-carbonate fraction, consisting of clay and/or organic matter. Given the fact that Sr^{2+} is relatively strongly adsorbed to phyllosilicates and organic matter, the presence of small amounts of non-carbonate fraction in a sample can increase the apparent $^{87}Sr/^{86}Sr$ values of carbonates (Burke et al., 1982), as clay minerals are enriched in radiogenic Sr. During sample dissolution dilute (1 M) hydrochloric acid was used to minimize the effect from any remaining clay/organic matter. Also, experiments with sample

Formatted: Superscript

Formatted: Superscript

Formatted: Font color: Auto

497 treatment procedures involving strong acid attack (see METHODS section) were evaluated by
498 dissolving some of the samples with 7 M HNO_3 instead of dilute HCl. These samples yield
499 $^{87}Sr/^{86}Sr$ ratios that are nearly-identical to those for samples leached with dilute HCl. Lastly, in
500 all of the limestone samples analysed, very little or no clay or organic residue was observed,
501 rendering Sr contamination from non-carbonate sources rather unlikely.
502
503 Renz and Habicht (1985) stated that the soft, unconsolidated pelagic sediments of the Blake–
504 Bahama Formation, cored at DSDP Site 534A in the western central Atlantic, form an
505 equivalent to the carbonate Maiolica facies in the Tethys (Bernoulli 1972, 2004). Similar to the
506 Blake Bahama Fm, the Maiolica limestones must have originated from soft, coccolith ooze. At
507 the sea floor, newly deposited calcareous ooze such as the Maiolica pelagic coccolith deposits
508 has an estimated porosity around 70% (Matter et al., 1975), with interstitial pore water
509 representing the chief component. In the Maiolica, the initially very high porosity was reduced
510 to zero during burial, either by (1) mechanical compaction and/or by (2) pore filling
511 cementation via pressure solution. Both are linked to the presence/absence of diagenetic fluid
512 pathways, and the stress caused by the load of the overburden during progressive burial. During
513 constant burial, porosity declines as a consequence of the load of the increasing overburden.
514 Furthermore, during pressure solution and subsequent pore-filling cementation, interstitial pore
515 waters will chemically reequilibrate with the surrounding carbonaceous ooze.
516
517 According to DePaolo and Finger (1991), recrystallization of soft, pelagic oozes should not
518 substantially modify the $^{87}Sr/^{86}Sr$ ratio of the sediment. This presumption arises from the fact
519 that during burial and lithification of calcareous ooze, diagenetic calcite is considered to be
520 obtained from local (pressure) dissolution-recrystallization (Jenkyns et al., 1995). As a result,
521 dissolution will deliver Sr to the pore fluids with an isotopic composition reflecting that of the

522 dissolving carbonate. Subsequent reprecipitation will then precipitate calcite that has the same
523 Sr isotope ratio as the pore fluid dissolved Sr. If dissolution-precipitation were the only
524 diagenetic process involved, the pore fluids and the carbonate would yield the same isotope
525 ratio at all depths, because the solid contains about 20 times more Sr than the pore fluid,
526 buffering the isotopic ratio of the seawater it was deposited from (Fantle and DePaolo, 2006).
527
528 However, an important matter to take into account is that high-porosity sediments such as
529 calcareous pelagic oozes are still in open, diffusive communication with the overlying seawater
530 (and porous sediment). Diffusional migration in pore waters is caused by differences in
531 concentration that develop between both sides of the sediment-water column interface (Lerman,
532 1978). Consequently, diffusion of aqueous Sr in the pore fluid will compete with the
533 dissolution-precipitation process, homogenizing pore fluid concentrations and isotope ratios
534 throughout the sediment column (Fantle and DePaolo, 2006).
535
536 Because the partition coefficient $D^{Sr}_{calcite} < 1$, the dissolution-reprecipitation of carbonates will
537 result in a net increase in Sr concentration in the pore waters (Baker et al, 1982). During
538 progressive burial and lithification, the Sr concentration in the pore waters will thus increase
539 with depth. Gieskes et al. (1986) emphasized that the peak in Sr concentrations is associated
540 with carbonate recrystallization reactions in the vicinity of the ooze-chalk transition, which
541 represents a diagenetic front in the sediment column. So, because the secular trend in Sr isotope
542 ratios throughout the Maiolica timeframe is one of constant increase (McArthur et al., 2001),
543 and because the down-gradient rate of Sr diffusion exceeds the rate of *in situ* recrystallization,
544 the water above the Sr concentration maximum is depleted, and that below enriched, in ^{87}Sr.
545 The *in situ* diagenetically precipitated carbonates then inherit this pore water Sr and shift the
546 bulk-rock isotopic composition toward that of the ambient pore waters.

Because the secular trend in Sr isotope ratios throughout the Maiolica timeframe is one of constant increase, before declining in the Mid-Barremmian, the $^{87}Sr/^{86}Sr$ ratios of the Maiolica carbonates ~~are~~ may have systematically displaced from that of the seawater in which it was deposited towards more radiogenic values. This is in accordance with modelling studies from Richter and De Paolo (1987), who developed a numerical model for the diagenetic exchange of Sr between chalks and their pore fluids during sedimentation and compaction in order to assess the accuracy with which the Sr isotope record in the carbonate sediment reflects that of seawater. Based on modelling studies, the authors postulate that for sediments older than 5 Ma the $^{87}Sr/^{86}Sr$ ratio of the carbonate is systematically displaced from that of the seawater in which it was deposited, with a maximum difference of +0.00005.

Considering this as an explanation for elevated $^{87}Sr/^{86}Sr$ compared to the global marine reference curve, diffusional migration and pore water exchange should also have affected the Sr isotopic signature in the upper part of the Maiolica succession, at least plateauing or ideally decreasing the $^{87}Sr/^{86}Sr$ at the respective stratigraphic interval. Our data show that the offset towards higher $^{87}Sr/^{86}Sr$ indeed seems to reach a plateau in the upper part of the section, although a decrease is not observed. Therefore it seems unlikely that diffusional migration was the only process affecting the $^{87}Sr/^{86}Sr$ of the Maiolica. During compaction, release of interlayer water from clays (in the small silicate fraction)-carrying a radiogenic $^{87}Sr/^{86}Sr$ signature, into to the pore water may have slightly offset the Sr isotopic composition if the pore water.

Both C and O isotopic data are in agreement with ~~theis~~the hypothesis of diffusional migration and pore water exchange. Carbon isotope ratios remain unchanged as they are buffered by the bicarbonate dissolved from the carbonate host. Contrary, although relative variations in the

oxygen isotopic record have remained unchanged, all values seem offset by approximately -1 ‰. Considering the geothermal gradient and the strong temperature-dependent fractionation of the oxygen isotopic system, this -1‰ shift to a more negative $\delta^{18}O$ value is a result of the roughly 5°C warmer temperatures at a burial depth of 50-250m, the depth at which gravitational compaction and dissolution-precipitation will- dominate the lithification process of calcareous oozes (Larsen and Chilingar, 1983~~).~~ ~~—~~Consequently, our Sr, O and C isotopic data support the hypothesis that the offset in $^{87}Sr/^{86}Sr$ results from incorporation of excess ^{87}Sr through isotopic reequilibration of carbonate with interstitial pore waters during progressive lithification of the calcareous ooze during diagenesis at slightly elevated temperatures.

4.2 The Weissert Event: constraints from Sr, O and C isotopic data

The Weissert Event has been recognized in Valanginian pelagic sediments of all the major oceans, including the Pacific (Weissert and Erba, 2004; Bartolini, 2003) and in shallow-water carbonate successions of the northern Tethys (Föllmi et al. 1994) and in fossil wood records (Gröcke et al. 2003). The Valanginian positive carbon isotope excursion thus seems to be of global extent and may serve as a useful stratigraphic marker (Weissert et al., 2008).

The Weissert Event is the first of ~~four~~ a series of Cretaceous excursions in the global $\delta^{13}C$ isotopic record.

The onset of the excursion in the Mid-Valanginian coincides with the onset of increased volcanic activity. This volcanism was essentially subaerial and localized in the Paranà–Etendeka province. Weissert and Erba (2004) suggested that the increase in atmospheric CO_2 resulting from increased subaerial volcanism may have caused accelerated weathering and

Formatted: Font color: Auto

hydrological cycling and thus indirect increased fertilization in coastal environments. Subsequent increased bioproductivity caused a drawdown of ^{12}C from the DIC reservoir in the oceans, increasing the $\delta^{13}C$ of the seawater, as recorded in authigenic marine carbonates.

Interestingly, there is isotopic and biotic evidence for a Valanginian cooling event coinciding with the time of the positive carbon isotopic excursion, based on (1) increased $\delta^{18}O$ values in marine carbonates, (2) the increase of boreal nannofossils in Romania (Melinte and Mutterlose, 2001) and (3) the occurrence of the nanofossil *Kokia borealis* in the equatorial Pacific (Weissert and Erba, 2004). Our data also show a peak in positive $\delta^{18}O$ values in the Maiolica at the base of the Valanginian carbon excursion (Fig. 4). This peak coincides with a shift in the Sr seawater curve to higher $^{87}Sr/^{86}Sr$. Interestingly, the $^{87}Sr/^{86}Sr$ peak we observe at the Weissert Event is not resolved by the Global Sr marine reference curve. However, the Sr marine reference curve assumes a global nature of the Sr-isotope signal. This assumption is true for modern major ocean basins that are well-connected with each other, yielding a relatively fast mixing time of 1500 years. However, it may not be an entirely valid assumption for past time-periods. Basins (such as the Umbria-Marche basin during the Early Cretaceous) might be relatively constricted, and if the size of the fluxes becomes much larger (with respect to the reservoir), the residence time of Sr may become shorter. This may play a role in the Sr excursions during extreme climate events, such as the Weissert Event.

Since elevated $^{87}Sr/^{86}Sr$ ratios in past oceanic seawater are a proxy for increased continental runoff, it can be regarded as a tool for tracing the causal connection between cycles of weathering and climatic perturbation, and the ~~paleo~~palaeobiotic response to these environmental changes. Although it must be emphasized that the climate-driven approach to global weathering (Ruddiman et al., 1997) is controversial and beyond the scope of this paper,

Formatted: Font color: Auto

Formatted: Font color: Auto

Formatted: Font color: Auto

Formatted: Font color: Auto

some interesting interpretations can be offered. The source of the weathering/climate connection is the atmospheric CO_2. It is thought that high CO_2 conditions in the atmosphere induce greater rainfall and temperatures, increasing the rate of continental chemical weathering, enhancing the flux of continental-derived (radiogenic) Sr to the oceans and increasing their $^{87}Sr/^{86}Sr$ (Ruddiman et al., 1997). In its turn, the process of weathering consumes the atmospheric CO_2, exerting a negative feedback ~~reaction~~ mechanism which triggers global cooling. In addition, increased continental runoff induces indirect fertilisation of the oceans, stimulating bioproductivity. This results in a drawdown of light ^{12}C from the oceans, and causes a positive shift in the $\delta^{13}C$ record. Elevated CO_2 levels may be explained by increased volcanic activity in the Paranà-Etendeka province during the Valanginian Weissert Event (Weissert and Erba, 2004). This hypothesis fits with elevated $^{87}Sr/^{86}Sr$, $\delta^{18}O$ and $\delta^{13}C$ values throughout the Valanginian.

An interesting observation is that the peak in the positive $\delta^{13}C$ excursion in the Valanginian post-dates both the strontium and oxygen isotopic shifts (Fig. 2) This contrasts with the observations of Weissert and Erba (2004), who state that the Valanginian cooling episode occurs within the *verrucosum* ammonite zone and should coincide with the heaviest $\delta^{13}C$ values. Considering our good biostratigraphic and magnetostratigraphic age control, the 'delayed' response of the carbon isotopic signal is likely a diagenetic artefact inherent to the Sr and O isotopic signals rather than a primary feature. In fact, it would seem that it is not the carbon signal that is delayed, but the Sr and O signatures that are shifted due to the diffusive communication of Sr from the pore waters in the overlying sediments and the seawater column into pore water during recrystallization-precipitation of the calcareous ooze. This process will

only affect the $\delta^{18}O$ and $^{87}Sr/^{86}Sr$ values, biasing their true stratigraphic, depositional age towards older ages, while the $\delta^{13}C$ system remains largely unaffected by this process.

Alternatively the positive spike in $\delta^{18}O$ and $^{87}Sr/^{86}Sr$ at the onset of the Weissert event can be explained by sample MMA11.2 being compromised by the vein calcite at the same stratigraphic level which is enriched in ^{18}O and ^{87}Sr. If one assumes the original geochemical data for MMA11.2 to be the average of MMA12 and MMA10, a 60:40 mix of bulk rock and vein calcite will generate the observed $\delta^{18}O$ and $^{87}Sr/^{86}Sr$ spikes. This admixture may not be in the form of ~~spariticsparry~~ calcite but may just be diffuse microcrystalline calcite formed within the rock matrix at the same time as the vein. However, we have sampled veins from other bulk rock samples (e.g. FRO 485.C, FRO 562.5C, PRE-3.C, Table 1). If we compare with the values for the host rock, the 87Sr/86Sr signature of the bulk is not biased towards more positive $\delta^{8}O$ and higher $^{87}Sr/^{86}Sr$, as is the case for sample MMA11. Therefore we believe this positive excursion in our 87Sr/86Sr record is a primary feature.

~~The theory of diffusive communication versus dissolution reprecipitation elegantly explains our systematic offset in Sr isotopic data from the seawater reference curve and the shift in the peak values of Sr and O isotopic excursions with respect to the $\delta^{13}C$ record throughout the Mid-Valanginian Weissert Event.~~

5. CONCLUSION

This study provides a composite record of $^{87}Sr/^{86}Sr$, $\delta^{18}O$ and $\delta^{13}C$ for three sections in the Tethyan Early -Cretaceous Maiolica sequence, carefully tied to a magnetostratigraphically and biostratigraphically calibrated timescale. The Sr isotope ratio record ~~accurately~~ follows the general trend of the ~~McArthur~~ Global Strontium~~r~~ isotope ratio seawater reference curve, though individual $^{87}Sr/^{86}Sr$ ~~isotope~~ ratios are systematically offset by +0.00007. We conclude that this

offset results from incorporation of excess ^{87}Sr through isotopic re-equilibration with interstitial pore waters during progressive compaction and lithification of the principal calcareous ooze, with a small contribution from calcite micro-veins. ~~Although the process occurs principally through dissolution-reprecipitation, buffering the contemporaneous seawater Sr isotopic signature, diffusional migration of Sr in pore waters is caused by differences in concentration that develop between the two sides of the sediment-water column interface (Lerman, 1978). Diffusive communication with the overlying water column and porous sediments will compete with the dissolution-precipitation process, homogenizing pore fluid concentrations and isotope ratios throughout the sediment column (Fantle and DePaolo, 2006). Because the secular trend in Sr isotope ratios throughout the Maiolica timeframe is one of constant increase, the $^{87}Sr/^{86}Sr$ ratios of the Maiolica carbonates are systematically displaced from that of the seawater in which it was deposited towards more radiogenic (higher $^{87}Sr/^{86}Sr$) values.~~

Furthermore, the (pristine) carbon isotope seawater record allows identification of the Mid-Valanginian Weissert event, characterized by a positive excursion in the $\delta^{13}C$ and the $\delta^{18}O$ record. In our record, the Weissert event correlates with a positive peak (+0.0001) in $^{87}Sr/^{86}Sr$. Both the Sr and O isotopic peaks pre-date the maximum peak in the $\delta^{13}C$ excursion. If we assume the excursion in the $\delta^{18}O$ and $^{87}Sr/^{86}Sr$ to reflect the oceanic conditions, ~~T~~this delay is likely a diagenetic artefact and further strengthens the hypothesis of diffusive communication of Sr with overlying water column during lithification of the calcareous ooze. ~~In addition, the Sr, O and C isotopic data seem to have recorded the apparent link between elevated (CO_2-driven) temperatures, increased chemical weathering, biotic response and negative feedback reactions.~~

The theory of diffusive communication versus dissolution-reprecipitation elegantly explains our systematic offset in Sr isotopic data from the seawater reference curve and the shift in the peak values of Sr and O isotopic excursions with respect to the $\delta^{13}C$ record in the Mid-Valanginian Weissert Event. In addition, this study highlights the importance of assessing the degree of diagenetic alteration using chemostratigraphic tools. In this context, it must be noted that the marine Sr reference curve (McArthur et al., 2001) is constructed based on measurement of (unaltered) low-Mg calcite shells instead of bulk carbonate rock. The reliability of the records therefore depends on how well unaltered forams/bivalves can be identified and separated. Richter and DePaolo (1987) stated that separates consisting of varying proportions of altered and unaltered forams may bias the data set, generating a source of noise that may hide the subtler aspects of $^{87}Sr/^{86}Sr$ variation with time in the ocean. On the other hand, it is expected that measuring the $^{87}Sr/^{S6}Sr$ of bulk carbonate data may lead to Sr isotopic signatures slightly deviating from the reference curve. However, contrary to the use of calcite shells, bulk carbonate data may generate less noisy data because of more consistent sampling. In summary, applying chemostratigraphy as a correlation tool must always be assessed in the light of the diagenetic processes involved, as the Sr isotopic curve of ~~paleo~~palaeoceans cannot be constrained better than that dictated by diagenetic considerations (Veizer, 1989).

6. ACKNOWLEDGEMENTS

Joke Belza acknowledges the Research Foundation Flanders (FWO) for its support in funding a PhD Fellowship. Alessandro Montanari and the Geological Observatory of Coldigioco provided logistical support during fieldwork. We thank John McArthur for sharing his Sr isotope ratio data in the early phases of this study. We thank Jim Channell for orientation data on his drill holes in the MMA section, and Bill Lowrie for orientation data on drill holes at FRO.

7. REFERENCES

Alvarez, W., 1989, Evolution of the Monte Nerone seamount in the Umbria-Marche Apennines: 1. Jurassic-Tertiary stratigraphy: Societá Geologica Italiana, Bollettino, v. 108, p. 3-21.

Alvarez, W., 2009, The historical record in the Scaglia limestone at Gubbio: magnetic reversals and the Cretaceous-Tertiary mass extinction: Sedimentology, v. 56, no. 1, p. 137-148.

Alvarez, W., Arthur, M. A., Fischer, A. G., Lowrie, W., Napoleone, G., Premoli Silva, I., and Roggenthen, W. M., 1977, Upper Cretaceous-Paleocene magnetic stratigraphy at Gubbio, Italy: V. Type section for the Late Cretaceous-Paleocene geomagnetic reversal time scale: Geological Society of America Bulletin, v. 88, p. 383-389.

Baker, P. A., Gieskes, J. M., and Elderfield, H., 1982, Diagenesis of carbonates in deep-sea sediments--evidence from Sr/Ca ratios and interstitial dissolved Sr^{2+} data: Journal of Sedimentary Petrology, v. 52, no. 71-82.

Bartolini, A., 2003, Cretaceous radiolarian biochronology and carbon isotope stratigraphy of ODP Site 1149 (Northwestern Pacific, Nadezhda Basin): Proceedings of the Ocean Drilling Program - Scientific Results, v. 185.

Bernoulli, D., 1972, North Atlantic and Mediterranean Mesozoic facies. : Initial Reports of the Deep Sea Drilling Project v. 11, p. 801-871.

Bernoulli, D., Gasperini, L., Bonatti, E., and Stille, P., 2004, Dolomite formation in Pelagic limestone and diatomite, Romanche Fracture Zone, equatorial Atlantic (Articolo in rivista): Journal of Sedimentary Research, v. 74, no. 6, p. 924-932.

Burke, W. A., Denison, R. E., Hetherington, E. A., Koepnik, R. B., Nelson, H. F., and Otto, J. B., 1982, Variation of seawater $^{87}Sr/^{86}Sr$ throughout Phanerozoic time: Geology, v. 10, p. 516-519.

Cecca, F., 1995, Late Valanginian ammonites from Monte Catria (Umbria-Marche Apennines, Italy): Memorie Descrittive della Carta Geologica d'Italia, v. 51, p. 47-57.

Cecca, F., Marini, A., Pallini, G., Baudin, F., and Begouen, V., 1994, A guide-level of the uppermost Hauterivian (Lower Cretaceous) in the pelagic succession of Umbria-Marche Apennines (Central Italy): The Faraoni Level: Rivista Italiana di Paleontologia e Stratigraphia, v. 99, no. 4, p. 551-568.

Channell, J. E. T., Cecca, F., and Erba, E., 1995, Correlations of Hauterivian and Barremian (Early Cretaceous) stage boundaries to polarity chrons: Earth and Planetary Science Letters, v. 134, p. 125-140.

Channell, J. E. T., Erba, E., and Lini, A., 1993, Magnetostratigraphic calibration of the Late Valanginian carbon isotope event in pelagic limestones from Northern Italy and Switzerland: Earth and Planetary Science Letters, v. 118, no. 1–4, p. 145-166.

Coccioni, R., Baudin, F., Cecca, F., Chiari, M., Galeotti, S., Gardin, S., and Salvini, G., 1998,, Integrated stratigraphic, palaeontological, and geochemical analysis of the uppermost Hauterivian Faraoni Level in the Fiume Bosso Section, Umbria-Marche Apennines, Italy: Cretaceous Research, v. 19, no. 1, p. 1-23.

Cresta, S., Monechi, S., Parisi, G., Baldanza, A., and Reale, V., 1989, Stratigrafia del Mesozoico e Cenozoico nell'area Umbro-Marchigiana/Mesozoic-Cenozoic stratigraphy in the Umbria-Marche area [in Italian and English]: Memorie Descrittive della Carta Geologica d'Italia, v. 39, no. 185.

De Muynck, D., Huelga-Suarez, G., Van Heghe, L., Degryse, P., and Vanhaecke, F., 2009, Systematic evaluation of a strontium-specific extraction chromatographic resin for obtaining a purified Sr fraction with quantitative recovery from complex and Ca-rich matrices: Journal of Analytical Atomic Spectrometry, v. 24, no. 11, p. 1498-1510.

DePaolo, D. J., and Finger, K. L., 1991, High-resolution strontium-isotope stratigraphy and biostratigraphy of the Miocene-Monterey-Formation, central California: Geological Society of America Bulletin, v. 103 no. 1, p. 112-124.

Field Code Changed

794 Edgar, K. M., Pälike, H., and Wilson, P. A., 2013, Testing the impact of diagenesis on the δ18O and δ13C
795 of benthic foraminiferal calcite from a sediment burial depth transect in the equatorial Pacific:
796 Paleoceanography, v. 28, no. 3, p. 468-480.
797 Fantle, M. S., and DePaolo, D. J., 2006, Sr isotopes and pore fluid chemistry in carbonate sediment of
798 the Ontong Java Plateau: Calcite recrystallization rates and evidence for a rapid rise in
799 seawater Mg over the last 10 million years: Geochimica et Cosmochimica Acta, v. 70, no. 15,
800 p. 3883-3904.
801 Faraoni, P., Flore, D., Marini, A., Pallini, G., and Pezzoni, N., 1997, Valanginian and early Hauterivian
802 ammonite successions in the Monte Catria group (Central Apennines) and in the Lessini Mts
803 (Southern Alps), Italy: Palaeopelagos, v. 7, p. 59-100.
804 Faure, G., and Powell, J. L., 1972, Strontium Isotope Geology, New York, Springer-Verlag, 188 p.:
805 Föllmi, K. B., Weissert, H., Bisping, M., and Funk, H., 1994, Phosphogenesis, carbon-isotope
806 stratigraphy and carbonate platform evolution along the northern Tethyan margin.: Geological
807 Society of America Bulletin, v. 106, p. 729-746.
808 Frijia, G., and Parente, M., 2008, Strontium isotope stratigraphy in the upper Cenomanian shallow-
809 water carbonates of the southern Apennines: Short-term perturbations of marine 87Sr/86Sr
810 during the oceanic anoxic event 2: Palaeogeography, Palaeoclimatology, Palaeoecology, v.
811 261, no. 1–2, p. 15-29.
812 Gieskes, J. M., Elderfield, H., and Palmer, M. R., 1986, Strontium and its isotopic composition in
813 interstitial waters of marine carbonate sediments: Earth and Planetary Science Letters, v. 77,
814 no. 2, p. 229-235.
815 Grippo, A., Fischer, A. G., Hinnov, L. A., Herbert, T. D., and Premoli SilvaI., I., 2004, Cyclostratigraphy
816 and chronology of the Albian stage (Piobbico core, Italy): Special Publication - Society for
817 Sedimentary Geology, v. 81, p. 57-81.
818 Gröcke, D. R., Price, G. D., Baraboshkin, E., Mutterlose, J., and Ruffell, A. H., 2003, The Valanginian
819 terrestrial carbon-isotope record: Geophysical Research Abstracts, v. 5
820 Grossman, E. L., 2012, Chapter 10 - Oxygen Isotope Stratigraphy, *in* Gradstein, F. M., Schmitz, J. G. O.
821 D., and Ogg, G. M., eds., The Geologic Time Scale: Boston, Elsevier, p. 181-206.
822 Hennig, S., Weissert, H., and Bulot, L., 1999, C-isotope stratigraphy, a calibration tool between
823 ammonite- and magnetostratigraphy: Geologica Carpathica, v. 50, p. 91-96.
824 Howarth, R. J., and McArthur, J. M., 1997a, Statistics for Strontium Isotope Stratigraphy: A Robust
825 LOWESS Fit to the Marine Sr-Isotope Curve for 0 to 206 Ma, with Look-up Table for Derivation
826 of Numeric Age: The Journal of Geology, v. 105, p. 441-456.
827 Howarth, R. J., and Mcarthur, J. M., 1997b, Statistics For Strontium Isotope Stratigraphy: A Robust
828 Lowess Fit to the Marine Sr-Isotope Curve For 0 to 206 Ma, With Look-Up Table For Derivation
829 of Numeric Age: The Journal of Geology, v. 105, no. 4, p. 441-456.
830 Jenkyns, H. C., Paull, K., Cummins, D. I., and Fullagar, P. D., 1995, Strontium-isotope stratigraphy of
831 lower Cretaceous atoll carbonates in the mid Pacific Mountains: Proceedings of the Ocean
832 Drilling Program - Scientific Results, v. 143, p. 89-97.
833 Larsen, G., and Chilingar, G. V., 1983, Diagenesis in Sediments and Sedimentary Rocks 2, Amsterdam,
834 Elsevier Scientific.
835 Lerman, A., 1978, Chemical Exchange Across Sediment-Water Interface: Annual Review of Earth and
836 Planetary Sciences, v. 6, p. 281-303.
837 Lowrie, W., and Alvarez, W., 1977, Upper Cretaceous-Paleocene magnetic stratigraphy at Gubbio, Italy:
838 III. Upper Cretaceous magnetic stratigraphy: Geological Society of America Bulletin, v. 1977, p.
839 374-377.
840 -, 1984, Lower Cretaceous magnetic stratigraphy in Umbrian pelagic limestone sections.: Earth and
841 Planetary Science Letters, v. 71, p. 315-328.
842 Lowrie, W., Alvarez, W., Premoli Silva, I., and Monechi, S., 1980, Lower Cretaceous magnetic
843 stratigraphy in Umbrian pelagic carbonate rocks: Geophysical Journal, v. 60, p. 263-281.

844 Madhavaraju, J., Lee, Y. I., and González–León, C. M., 2013, Diagenetic significance of carbon, oxygen
845 and strontium isotopic compositions in the Aptian-Albian Mural Formation in Cerro Pimas
846 area, northern Sonora, Mexico: Journal of Iberian Geology v. 39 no. 1, p. 73-88.
847 Maliva, R. G., and Dickson, J. A. D., 1997, Ulster white limestone formation (Upper Cretaceous)of
848 Northern Ireland: effects of basalt loading on chalk diagenesis: Sedimentology v. 44, no. 105-
849 112.
850 Maliva, R. G., Dickson, J. A. D., Smalley, P. C., and Oxtoby, N. H., 1995, Diagenesis of the Machar field
851 (British North-Sea) chalk: evidence for decoupling of diagenesis in fractures and the host rock:
852 Journal of Sedimentary Research v. 65, no. 105-111.
853 Marshall, J. D., 1992, Climatic and oceanographic isotopic signals from the carbonate rock record and
854 their preservation: Geological Magazine, v. 129, no. 143-160.
855 Matter, A., Douglas, R. G., and Perch-Nielson, K., 1975, Fossil preservation, biochemistry, and
856 diagenesis of pelagic carbonates from Shatsky Rise, northwest Pacific: Proceedings of the
857 Ocean Drilling Program, Initial Reports, no. 32, p. 891-907.
858 McArthur, J. M., Howarth, R. J., and Bailey, T. R., 2001, Strontium Isotope Stratigraphy: LOWESS Version
859 3: Best Fit to the Marine Sr-Isotope Curve for 0–509 Ma and Accompanying Look-up Table for
860 Deriving Numerical Age: The Journal of Geology, v. 109, p. 155–170.
861 McArthur, J. M., Howarth, R. J., and Shields, G. A., 2012, Chapter 7 - Strontium Isotope Stratigraphy, *in*
862 Gradstein, F. M., Schmitz, J. G. O. D., and Ogg, G. M., eds., The Geologic Time Scale: Boston,
863 Elsevier, p. 127-144.
864 Melinte, M., and Mutterlose, J., 2001, A Valanginian (Early Cretaceous) 'Boreal nannoplankton
865 excursion' in sections from Romania: Marine Micropaleontology, v. 43, p. 1-25.
866 Montanari, A., and Koeberl, C., 2000, Impact stratigraphy: the Italian record, *in* Bhattacharji, S.,
867 Friedman, G. M., Neugebauer, H. J., and Seilacher, A., eds., Lecture Notes in Earth Sciences,
868 Volume 93: Berlin, Springer Verlag, p. 364.
869 Palmer, M. R., and Edmond, J. M., 1989, The strontium isotope budget of the modern ocean: Earth and
870 Planetary Science Letters, v. 92, no. 1, p. 11-26.
871 Renz, O., and Habicht, K., 1985, A correlation of the Tethyan Maiolica Formation of the Breggia section
872 (southern Switzerland) with Early Cretaceous oozes of Site 534A, DSDP Leg 76 in the western
873 Atlantic: Eclogae Geologicae Helvetiae, v. 78 no. 2 p. 383-431.
874 Richter, F. M., and DePaolo, D. J., 1987, Numerical models for diagenesis and the Neogene Sr isotopic
875 evolution of seawater from DSDP Site 590B: Earth and Planetary Science Letters, v. 83, no. 1–
876 4, p. 27-38.
877 Rohling, E. J., and Bigg, G. R., 1998, Paleosalinity and δ18O: A critical assessment: Journal of
878 Geophysical Research: Oceans, v. 103, no. C1, p. 1307-1318.
879 Ruddiman, W. F., Kutzbach, J. E., and Prentice, C., 1997, Testing the climatic effects of orography and
880 CO_2 with general circulation and biome models, *in* Ruddiman, W. F., ed., Tectonic uplift and
881 climate change: New York, Plenum Press, p. 203-235.
882 Schrag, D. P., DePaolo, D. J., and Richter, F. M., 1995, Reconstructing past sea surface temperatures:
883 Correcting for diagenesis of bulk marine carbonate: Geochimica et Cosmochimica Acta, v. 59,
884 no. 11, p. 2265-2278.
885 Shackleton, N., 1967, Oxygen Isotope Analyses and Pleistocene Temperatures Re-assessed: Nature, v.
886 215, no. 5096, p. 15-17.
887 Sprovieri, M., Coccioni, R., Lirer, F., Pelosi, N., and Lozar, F., 2006, Orbital tuning of a Lower Cretaceous
888 composite record (Maiolica Formation, central Italy): Paleoceanography, v. 21, no. 4, p. 19.
889 Sundquist, E. T., and Visser, K., 2003, 8.09 - The Geologic History of the Carbon Cycle, *in* Turekian, H.
890 D. H. K., ed., Treatise on Geochemistry: Oxford, Pergamon, p. 425-472.
891 Thirlwall, M. F., 1991, Long-term reproducibility of multi-collector Sr and Nd isotope ratio analysis:
892 Chemical Geology, v. 94, p. 85-104.
893 Veizer, J., 1989, Strontium Isotopes in Seawater through Time: Annual Review of Earth and Planetary
894 Sciences, v. 17, no. 1, p. 141-167.

Veizer, J., Ala, D., Azmy, K., Bruckschen, P., Buhl, D., Bruhn, F., Carden, G. A. F., Diener, A., Ebneth, S., Godderis, Y., Jasper, T., Korte, C., Pawellek, F., Podlaha, O. G., and Strauss, H., 1999, $^{87}Sr/^{86}Sr$, $\delta^{13}C$ and $\delta^{18}O$ evolution of Phanerozoic seawater: Chemical Geology, v. 161, no. 1-3, p. 59-88.

Veizer, J., Fritz, P., and Jones, B., 1986, Oxygen and carbon isotopic records of Paleozoic oceans: Geochimica et Cosmochimica Acta, v. 50, p. 1679-1696.

Weissert, H., and Erba, E., 2004, Volcanism, CO_2 and palaeoclimate: a Late Jurassic–Early Cretaceous carbon and oxygen isotope record: Journal of the Geological Society, v. 161, no. 4, p. 695-702.

Weissert, H., Joachimsky, M., and Sarnthein, M., 2008, Chemostratigraphy: Newsletters on Stratigraphy, v. 42, no. 3, p. 145-179.

Weissert, H., McKenzie, J. A., and Channell, J. E. T., 1985, Natural variations in the carbon cycle during the Early Cretaceous, *in* Sundquist, E. T., and Broeker, W. S., eds., The Carbon Cycle and Atmospheric CO_2: Natural Variations Archean to Present Volume 32, American Geophysical Union, p. 531-545.

Weissert, H. and Channell, J.E.T. , 1989, Tethyan carbonate carbon isotope stratigraphy across the Jurassic-Cretaceous boundary: an indicator of decelerated carbon cycling. : Paleoceanography, v. 4, p. 483-494.

Zeebe, R. E., and Wolf-Gladrow, D., 2001, CO_2 in seawater: Equilibrium, kinetics, isotopes, Amsterdam, Elsevier, Elsevier Oceanography Series.

FIGURE CAPTIONS

Figure 1. Locality map for the sections sampled in this study: Frontale (FRO) Presale (PRE) and Monte Acuto (MMA)

Figure 2. The upper Valanginian portion of the Maiolica exposed at the MMA section. The section in this view extends about 40 m along the road, and the beds dip southwest, on the southwest flank of the Monte Acuto-Monte Catria anticline; the center of the photo is at 43° 27.828'N, 12° 40.380'E.

Formatted: Font color: Auto

Formatted: Font color: Auto

Figure 3. Isotopic data and age calibration for the Maiolica of the Monte Acuto, Frontale and Presale stratigraphic sections. GTS 2012 = Geologic Time Scale 2012 (Gradstein et al., 2012). For details of the polarity zonation, see Ogg, 2012, GTS 2012, Table 5.2. For the Tethyan ammonite zonation, see Ogg and Hinov, 2012, GTS 2012, p. 813

Figure 4. Composite curve $^{87}Sr/^{86}Sr$, $\delta^{18}O$ and $\delta^{13}C$ for the Monte Acuto stratigraphic section. Samples are plotted with equal spacing. ~~Samples are equally spaced; this not a linear age scale.~~

~~Figure 5. Cross-plot of $\delta^{13}C$ versus $\delta^{18}O$ of bulk carbon and oxygen isotopic values for MMA, FRO and PRE sections and linear regression fit (dashed lines). The low covariance between $\delta^{13}C$ and $\delta^{18}O$ (R^2= 0.0030-0.4) hints towards minimal diagenetic modification.~~

Formatted: Font color: Auto